Publisher's PDF, also known as Version of record

License (if available):
CC BY

Link to published version (if available):
[10.1144/SP420.12](10.1144/SP420.12)

Link to publication record in Explore Bristol Research
PDF-document

University of Bristol - Explore Bristol Research
General rights

Influence of regional tectonics and pre-existing structures on the formation of elliptical calderas in the Kenyan Rift

E. A. M. ROBERTSON[1]*, J. BIGGS[1], K. V. CASHMAN[1],
M. A. FLOYD[2] & C. VYE-BROWN[3]

[1]*School of Earth Sciences, University of Bristol, Wills Memorial Building,
Queen's Road, Bristol BS8 2JN, UK*

[2]*Department of Earth, Atmospheric and Planetary Sciences, Massachusetts Institute of
Technology, Cambridge, MA, USA*

[3]*British Geological Survey, Murchison House, West Mains Road, Edinburgh EH9 3LA, UK*

*Corresponding author (e-mail: elspeth.robertson@bristol.ac.uk)

Abstract: Calderas are formed by the collapse of large magma reservoirs and are commonly elliptical in map view. The orientation of elliptical calderas is often used as an indicator of the local stress regime; but, in some rift settings, pre-existing structural trends may also influence the orientation. We investigated whether either of these two mechanisms controls the orientation of calderas in the Kenyan Rift. Satellite-based mapping was used to identify the rift border faults, intra-rift faults and orientation of the calderas to measure the stress orientations and pre-existing structural trends and to determine the extensional regime at each volcano. We found that extension in northern Kenya is orthogonal, whereas that in southern Kenya is oblique. Elliptical calderas in northern Kenya are orientated NW–SE, aligned with pre-existing structures and perpendicular to recent rift faults. In southern Kenya, the calderas are aligned NE–SW and lie oblique to recent rift faults, but are aligned with pre-existing structures. We conclude that, in oblique continental rifts, pre-existing structures control the development of elongated magma reservoirs. Our results highlight the structural control of magmatism at different crustal levels, where pre-existing structures control the storage and orientation of deeper magma reservoirs and the local stress regime controls intra-rift faulting and shallow magmatism.

Supplementary material: Details of the Standard Deviation Ellipse function and statistical methods are available at http://www.geolsoc.org.uk/SUP18849

The evolution of a continental rift is influenced by faulting and the intrusion, transport and eruption of melts (e.g. McKenzie 1978). As such, there is a close relationship between magmatism and the crustal and/or local stress field. The surface expression of volcanism often exhibits features associated with crustal and local stresses. These include elliptical calderas, vent alignment and the orientation of dykes. The Kenyan Rift is an immature section of the East African Rift System (EARS) (Ebinger 2005), where lithospheric thinning occurs by a combination of faulting and magmatism, as indicated by large offset border faults, silicic caldera volcanoes and the extensive lavas that comprise the rift floor (Pointing *et al.* 1985; Young *et al.* 1991; Latin *et al.* 1993; Tongue *et al.* 1994; Ibs-von Seht *et al.* 2001).

There are seven silicic caldera volcanoes in the Kenyan Rift (Fig. 1), all of which are elliptical in map view with varying orientations. This study investigated whether the local contemporary stress regime or pre-existing structures control caldera orientation in the Kenyan Rift. Understanding the caldera orientation gives us important information about the structural controls on magmatic and tectonic behaviour in extensional settings and the mechanisms by which continental rifts evolve from fault-controlled basins into mid-ocean ridges (MORs).

Calderas

Calderas are volcanic collapse features related to the withdrawal of magma from an underlying reservoir (Williams 1941; Smith & Bailey 1968; Druitt & Sparks 1984; Lipman 1984; Branney 1995; Cole *et al.* 2005). Worldwide, and across all tectonic settings, the majority of calderas are elliptical. Moreover, those calderas that appear near-circular are
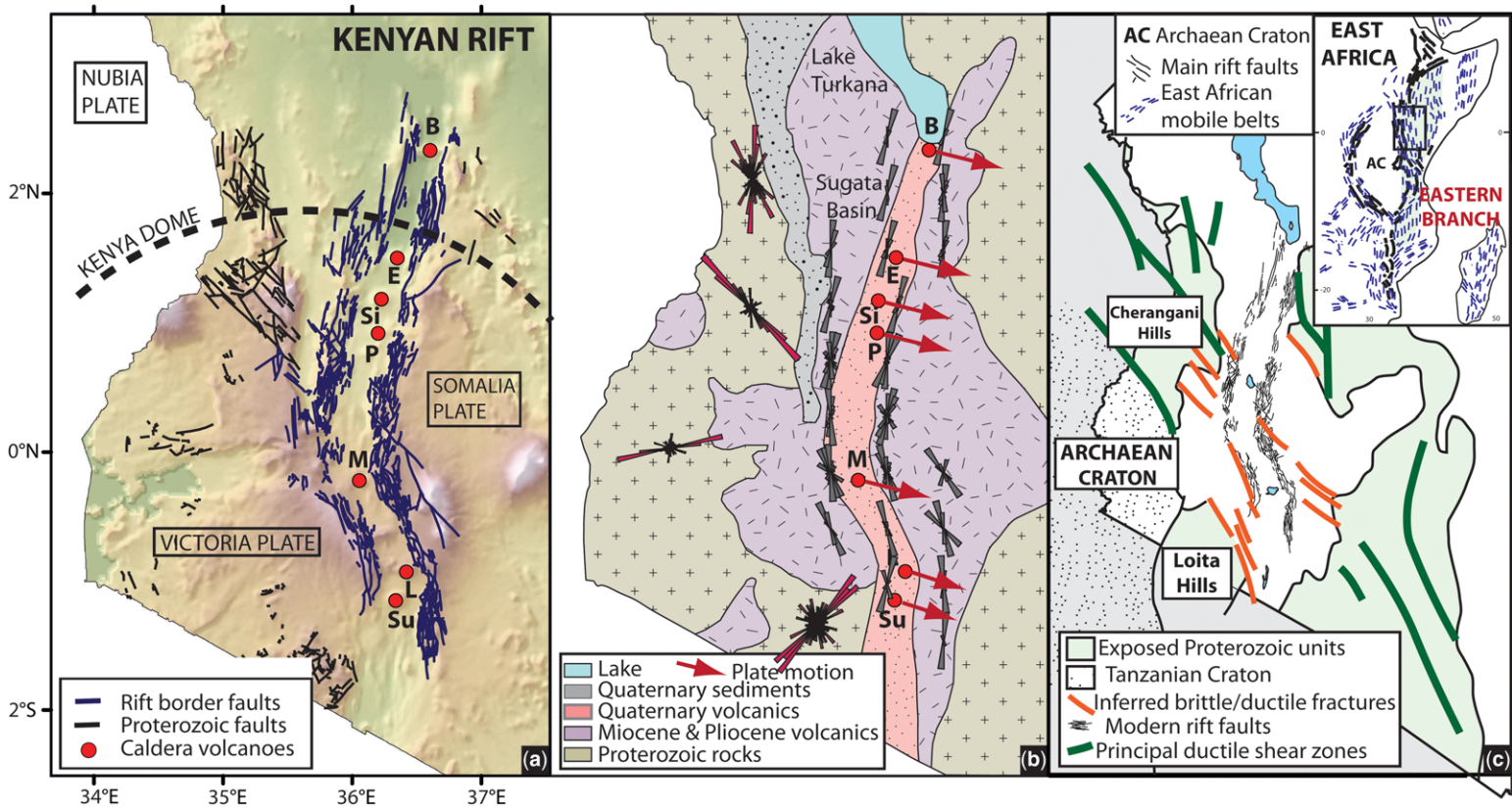
Fig. 1. Location map of the Kenyan Rift showing its geology and structure. Location of Quaternary caldera volcanoes (red circles) are labelled as: B, the Barrier; E, Emuruangogolak; Si, Silali; P, Paka; M, Menengai; L, Longonot; and Su, Suswa. (**a**) Digital Elevation Map showing the location of the rift border faults and major faults exposed in the Proterozoic units. Approximate northern extent of the Kenyan Dome is marked. (**b**) Summary geological map of Kenya after BEICIP (1987). Red arrows show the motion of the Somalia plate relative to the Victoria plate calculated at each caldera volcano with Euler poles from Stamps *et al.* (2008). Grey rose diagrams show the length-weighted orientation of the main rift border faults calculated in half-degree segments. Pink rose diagrams show the orientation of faults formed in the Proterozoic. (**c**) Exposure of Kenyan Proterozoic units and principal structures, adapted from Mosley (1993). The Proterozoic exposures form part of the East African Mozambique Mobile Belt (inset). Major sinistral ductile shear zones and inferred brittle/ductile fractures are shown and were formed during a distinct tectonothermal collisional episode 630–580 Ma. Cherangani and Loita Hills are referenced in the text; these locations have exposed faulting resulting from the collisional episode. Inset based on Vauchez *et al.* (2005).

E. A. M. ROBERTSON *ET AL.*

rarely perfectly rounded (Holohan *et al.* 2005; Spinks *et al.* 2005; Gudmundsson 2007). Elliptical calderas may form as a result of a combination of factors, such as the magma reservoir geometry, regional tectonics and regional structures. Elliptical calderas are common across all extensional settings, including Iceland, New Zealand and the EARS (Wilson *et al.* 1995; Bosworth *et al.* 2000; Acocella *et al.* 2002; Holohan *et al.* 2005).

Holohan *et al.* (2005) suggested four mechanisms that can produce elliptical calderas (Table 1).

(1) An elongated magma reservoir: the collapse of an elliptical magma reservoir produces an elliptical caldera. Elliptical magma reservoirs may align with either the maximum or minimum horizontal stress (e.g. Bosworth *et al.* 2003) or with a pre-existing anisotropy such as a fault or fracture system (Acocella *et al.* 2002).

(2) Nesting: successive collapse of intersecting calderas over time produces nested structures that appear elliptical in plan view. The formation of a nested caldera is usually attributed to the development of a new shallow magmatic system, which is offset from the older system (Geyer & Martí 2009).

(3) Shallow crustal processes: assuming that the magma reservoir is spherical, the distortion of caldera ring faults during collapse influences the caldera geometry. Processes and structures that may affect caldera ring fault location include shallow crustal faults, asymmetrical subsidence during collapse, the pre-collapse topography and variable loading on the magma reservoir.

(4) Post-caldera processes: an originally near-circular caldera becomes elliptical over time as a result of erosion of the caldera walls or by the spalling of caldera wall rock as a result of the formation of shear fractures sub-parallel to the current day crustal stress orientation.

Extensional tectonic settings

A common feature of rifts is that the plate motion is typically oblique to the plate boundary (Dewey *et al.* 1998; Fossen & Tikoff 1998). The angles between the plate motion vector, the plate margin orientation and the orientation of extensional faults can be used to classify the type of extension as oblique opening, short-segment opening (not observed in nature and therefore not discussed here), transtension and orthogonal opening (Tuckwell *et al.* 1996; Fig. 2).
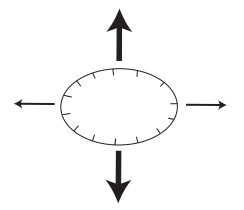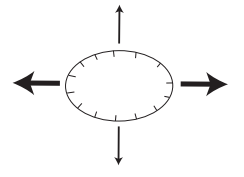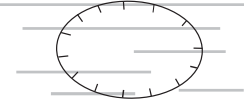
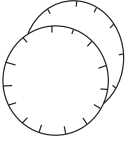In orthogonal opening (Fig. 2b), both extensional faults (intra-rift faults in a continental rift setting)
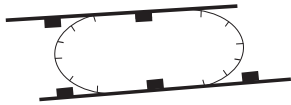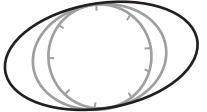
and the plate margin (rift border faults in a continental rift setting) are normal to the plate motion vector. This situation occurs frequently in extensional settings, particularly at MORs. Oblique opening (Fig. 2c) occurs when intra-rift faults form parallel to the plate margin; the plate motion vector is oblique to both. Transtension (Fig. 2d) describes the situation where the plate margin, extensional faults and the plate motion vector are all oblique to one another. Geometrically, transtension is where extensional faults form normal to the local minimum principal stress, but oblique to both the plate motion vector and the plate margin. This criteria fulfils $\phi = A/2$ and $\varphi = \alpha/2 + 45°$, where ϕ is the angle between the plate margin and the extensional faults, A is the angle between the plate motion vector and the normal to the plate margin, and φ and α are the angles between the plate motion vector and the extensional faults and plate margin, respectively (Tuckwell *et al.* 1996).

These divergent plate margin models have largely been applied at MOR settings, primarily to explain the orientation of faults at MORs and to investigate morphological variations with the spreading rate (Tuckwell *et al.* 1996; Wormald *et al.* 2012). However, they have also been applied at continental rift settings such as the Main Ethiopian Rift (MER) (S.C. Wormald, pers. comm. 2013), from which this work is inspired. These studies showed that both transtension and orthogonal spreading are the dominant style of extension at both MORs and continental rifts globally. For MORs, the spreading rate exerts an important control on the type of extension: slow-spreading ridges (half-rate <20 mm a^{-1}) are more often in transtension and fast-spreading ridges more often show orthogonal opening (Tuckwell *et al.* 1996).

The relationship between plate motion, intra-rift faults and rift border faults at continental rift settings is typically more complex than at MORs. For instance, during extension, pre-existing zones of lithospheric weakness can localize deformation, which, in turn, can cause rift border faults to form oblique to the stretching direction. An exception is the case where a pre-existing zone of weakness is orthogonal to the stretching direction (Agostini *et al.* 2009; Philippon *et al.* 2015). This is identified in both analogue studies and at natural oblique rifts (Agostini *et al.* 2009; Corti 2012; Corti *et al.* 2013). Further complexity is observed in the MER, where the reactivation of pre-existing lithospheric weaknesses during extension has led to the development of rift border faults that are oblique to both the main rift trend and the extension direction (e.g. Agostini *et al.* 2011). For MER segments that have a low/moderate obliquity angle between the rift trend and the extension orientation ($15–45°$), the intra-rift fault orientation tends to form orthogonal to the

Table 1. *Mechanisms for elliptical caldera formation in extensional settings*

Mechanism	Theory of elongation	Example	Long axis alignment
1. Elongated magma reservoirs	Caldera ellipticity reflects elongation of underlying magma body*		
(a) Aligned to minimum horizontal compressional stress orientation	Mechanism analogous to borehole break-out where the magma reservoir wall becomes elongated parallel to the minimum horizontal stress due to stress-induced spalling of the magma reservoir wall	Long Valley, USA[1]	
(b) Aligned to maximum horizontal compressional stress orientation	Orientation is controlled by the regional tectonic trend, either by faults that are accommodating extension or through the development of a dyke-like feature	–	
(c) Aligned to pre-existing anisotropy at a similar depth to the magma reservoir	Pre-existing structures are exploited during extension. Faults are not necessarily exposed at the surface directly adjacent to caldera and faults are not necessarily parallel to the current extensional regime	Gariboldi, Ethiopia[2]; Kapenga, New Zealand[3]	

2. Nested	Nested or overlapping calderas are associated with several discrete eruptions and collapse events due to the development of new magma reservoirs	Campi Flegrei, Italy[4]; Pantelleria, Italy[5]	
3. Shallow crustal processes	Caldera geometry is altered in the shallow crust due to the influence of localized stresses or faults and fractures*		
(a) Aligned to active (extensional) structures in the crust	Local pre-existing stresses due to extension within the shallow crust creating zones of weakness, faults or fractures that affect caldera ring fault orientation	Okataina, NZ[6]	
(b) Distorted due to local faults, asymmetrical subsidence or topography	(i) Regional shallow faults exert control on caldera ring fault location	Ranau, Indonesia[7]	
	(ii) Asymmetrical subsidence on linear or arcuate faults during caldera formation	Toba, Indonesia[8]	
	(iii) Pre-collapse topography and variable loading on magma reservoir roof	Rotorua, New Zealand[9]	
4. Post-caldera formation processes	Original caldera structure is altered due to post-collapse erosional processes or continued regional strain	Aso, Japan[10]*	

*Assuming the magma reservoir geometry is spherical. Based on Holohan *et al.* (2005).
References: 1, Moos & Zoback (1993); 2, Acocella *et al.* (2002); 3 and 6, Spinks *et al.* (2005); 4, Orsi *et al.* (1996); 5, Mahood & Hildreth (1986); 7 and 8, Bellier & Sébrier (1994); 9, Spinks *et al.* (2005); and 10*. Sudo & Kong (2001) – also formed in conjunction with multiple eruptions.
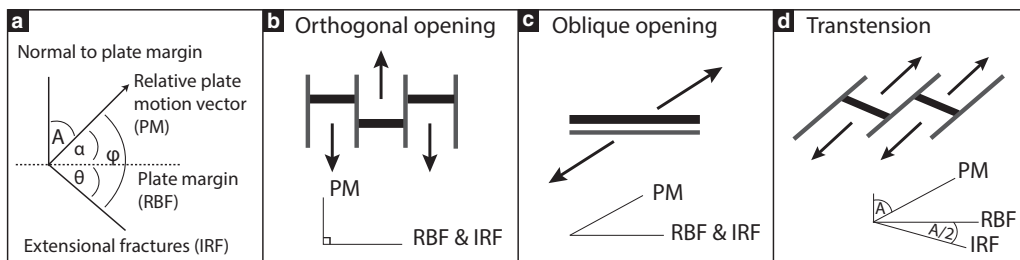
Fig. 2. Models for the orientation of extensional fractures at diverging tectonic margins with respect to the relative plate motion vector and the plate margin orientation. Element descriptions are adapted for a continental rift setting therefore extensional fractures become intra-rift faults and the plate margin orientation is represented by rift border faults. (**a**) Geometrical relationship between the structural elements used in the models. (**b, c, d**) The three models presented are orthogonal opening, oblique extension and transtension. Modified from Tuckwell *et al.* (1996).

extension direction (Agostini *et al.* 2009; Corti 2012). As a result of this complexity, rift kinematics in the MER are typically defined on the basis of the rift trend orientation with respect to the plate motion vector (e.g. Corti 2012). Orthogonal rifting is thus defined when extension is normal to the rift trend, low/moderate obliquity occurs when $\alpha \leq 45°$ (where α is the obliquity angle, i.e. the angle between the direction of extension and the orthogonal to the rift trend) and high obliquity rifts occur when $\alpha \geq 45°$.

Volcanic proxies for tectonic stress orientation

Elliptical calderas are often used as an indicator of far-field tectonic stress orientation, whereby the long axis aligns parallel to the minimum horizontal stress orientation (Bosworth *et al.* 2003; Wormald *et al.* 2012). Consequently, elongated calderas have been used to reconstruct past directions of regional extension (Wallmann *et al.* 1990; Bosworth *et al.* 2003; Holohan *et al.* 2005; Casey *et al.* 2006). However, caldera elongation may not always be a reliable proxy for stress orientation as studies show that the long axes of calderas may also align with pre-existing fault systems (Acocella *et al.* 2002; Spinks *et al.* 2005).

Dykes are considered to be a robust indicator of stress field orientation because both field observations and modelling show that intrusions propagate parallel to the maximum horizontal stress (Nakamura 1977; Delaney *et al.* 1986). Consequently, dyke orientation has been used to infer both past and present stress orientations (Nakamura 1969, 1977; Delaney *et al.* 1986; Pollard 1987; Rubin 1995; Rowland *et al.* 2010). In addition, linear alignments of volcanic vents, cinder cones, domes and pyroclastic cones can also be used to reconstruct the stress field orientation if they originate from

feeder dykes (Nakamura 1969, 1977; Gudmundsson 1995, 2005; Korme *et al.* 1997).

Tectonic and volcanic setting

Regional tectonic setting

The EARS extends from the Afar triple junction and the Red Sea to Mozambique, delineating the divergent boundary between the Nubia and Somalia plates (Fig. 1). On a broad scale, the EARS overlies one of the most extensive seismic velocity anomalies in the upper mantle, the African superswell (e.g. Nyblade & Robinson 1994; Ritsema *et al.* 1999; Kendall *et al.* 2006), which is responsible for a topographic high that includes southern Africa and southwestern Arabia (Daradich *et al.* 2003) and the localized uplifted areas known as the Kenyan and Ethiopian domes (Davis & Slack 2002). The EARS splits into two branches, the Eastern Branch and the Western Branch, around the Archaean Craton, constituting the Victoria plate (Fig. 1c, inset).

Within Kenya, the EARS is often referred to as the Kenyan (or Gregory) Rift. It follows the general north–south trend of the Mozambique Mobile Belt, a Proterozoic metamorphic collision orogen extending through East Africa (Shackleton 1984; Shackleton & Ries 1984), as it passes through the topographic high of the Kenya Dome (Fig. 1a). The Kenyan Rift forms a series of fault-bound graben with major normal faults arranged en echelon (Baker & Wohlenberg 1971). Although the main trend of the Kenyan Rift lies north–south, the orientations of individual rift segments vary. For example, in the Turkana region of northern Kenya, rift border faults are orientated NNE–SSW before shifting to a NNW–SSE direction; towards Tanzania, rift border faults return to a north–south/NNE–SSW orientation (Fig. 1b). The horizontal stress field in Kenya is inferred as having rotated anticlockwise

from east–west to NW–SE at *c.* 600 ka (Strecker *et al.* 1990; Strecker & Bosworth 1991).

Rifting in Kenya initiated at *c.* 25 Ma, concurrent with the extrusion of extensive basaltic lava flows in northern Kenya (Ebinger 1989). Northern Kenya has extended by 35–40 km (Hendrie *et al.* 1994), in contrast with 4–20 km of extension in central and southern Kenya (Baker *et al.* 1972). The crustal thickness varies from 20 km at *c.* 3°N to 35 km at the Equator (Prodehl *et al.* 1997). A partially molten upper mantle may underlie the Kenyan Rift, as suggested by low seismic velocities, and may possibly form a series of fractionated magmatic intrusions (Achauer 1992; Achauer *et al.* 1994; Birt *et al.* 1997; Thybo *et al.* 2000; Achauer & Masson 2002).

Pre-existing lithospheric anisotropies have influenced the location and propagation of the EARS (McConnell 1972; Chorowicz *et al.* 1987; Daly *et al.* 1989; Fairhead & Green 1989; Versfelt & Rosendahl 1989; Chorowicz 2005). Furthermore, Proterozoic lithospheric structures associated with the mobile belts may have controlled the initial evolution of the EARS (Bastow *et al.* 2008; Keranen & Klemperer 2008; Keranen *et al.* 2009).

Proterozoic structures

The Proterozoic Mozambique Mobile Belt is a broad north–south zone of polyphase metamorphic structures extending throughout Eastern Africa and is bounded to the west by the Archaean Craton (Mosley 1993; Hetzel & Strecker 1994; Fig. 1c inset). The current view is that the craton has been reworked and overthrust on the Mozambique Mobile Belt and that the original contact position is *c.* 100 km east and NE of the exposed contact (Mosley 1993; Smith & Mosley 1993).

In Kenya, a Cambrian–Ordovician collisional event (530–430 Ma) produced sinistral NW–SE-trending upright shear zones and a conjugate NE–SW weaker shear set (Fig. 1c). These shear zones appear to reflect major crustal and/or lithospheric weaknesses that have subsequently controlled the evolution of the EARS (Mosley 1993; Braile *et al.* 1995).

The major Proterozoic NW–SE shear zones have been identified and mapped on both rift shoulders, but recent Mesozoic and Quaternary volcanic and sedimentary deposits mostly cover these zones within the rift. In northern Kenya, surrounding the Cherangani Hills, the exposed belt consists of thick quartzites and massive limestones; dominant NW–SW faults were formed during the 530–430 Ma collision event. In southern Kenya, near the Loita Hills, quartzites and semi-pelitic gneisses dominate. All units have been subject to heavy tectonism, with major recumbent folding and thrusting,

probably from the collision with the nearby Tanzanian craton. In this location, early recumbent folds have NE-trending hinges, but have since been refolded on NW axes. At least four fault populations have been identified: normal north–south; dextral NW–SE; strike-slip ENE–WSW; and sinistral NE–SW. Of these, the NW–SE and NE–SW sets are currently active (Kuria *et al.* 2010).

Although the crustal structure is likely to have been deformed during rifting, published evidence supports the view that Precambrian features persist beneath the rift and have controlled the ascent of magma. Mugisha *et al.* (1997) suggested that Precambrian shear zones have influenced rift basin geometries and Mosley (1993) proposed that a network of these Proterozoic structures beneath the rift affects the magma plumbing and the rate of ascent and emplacement of magma bodies in the upper crust. Furthermore, Key *et al.* (1989) identified joint systems that may have acted as magma conduits, as interpreted by Haug & Strecker (1995).

Volcanic setting

Fifteen Quaternary volcanoes line the central axis of the Kenyan Rift, seven of which have visible caldera collapse structures. Geographically, the caldera volcanoes can be separated into two groups: a northern group that includes the Barrier, Emuruangogolak, Silali and Paka volcanoes and a southern group that includes Menengai, Longonot and Suswa (McCall 1968; Williams 1978*a*, *b*; Williams *et al.* 1984). The major volcanological features are described in Table 2.

Although there are no historical records of eruptions, ground displacement has been observed at five Kenyan volcanoes (Biggs *et al.* 2009, 2013), with subsidence at Suswa and Menengai from 1997 to 2000, uplift at Paka and Longonot throughout 2006–07 and 2004–06, and slow subsidence at Silali between 2007 and 2010 (Fig. 3). The deformation observed at Suswa, Menengai, Longonot and Paka volcanoes was episodic (Biggs *et al.* 2009), but further results suggest that slow subsidence is occurring at Silali (Biggs *et al.* 2013). The source of deformation at all edifices is shallow, with modelled source depths between 0.7 and 4.1 km.

The ages of the volcanoes range from *c.* 1300 ka at the Barrier complex to *c.* 240 ka at Suswa volcano (Table 2). Each volcano consists of a single, shield-shaped edifice, with the exception of the Barrier, which is a complex of four overlapping volcanoes (Kalolenyang, Kakorinya, Likaiu West and Likaiu East) that forms a 20 × 15 km physical barrier between Lake Turkana and the Suguta Basin (Dunkley *et al.* 1993). Although caldera collapse occurred at Kakorinya summit, we refer to this caldera as the Barrier, in keeping with previously

Table 2. *Summary of volcanological data for Kenyan caldera volcanoes*

Volcano	Location	Age (ka)	Dominant composition	Caldera			Collapse mechanism
				Age (ka)	Size (km) and orientation		
The Barrier	2.32° N 36.57° E	1300	Trachyte and phonolite lavas, basalt fissure eruptions[1,2,3,4,5]	58–92	3.8	ESE	Unknown; tentatively associated with a pumice deposit
Emuruangogolak	1.5° N 36.33° E	500–900	Trachyte and basaltic shield lavas and trachyte pyroclastics, extensive dyking resulting in basaltic fissures and cones[3,6,7,8,9]	38 ± 6	5 × 3.5	ESE	Unknown; dated after flank eruptions of trachytes and pyroclastics that may or may not be associated with collapse
Silali	1.15° N 36.23° E	225–400	Trachyte and basaltic lavas and trachyte pyroclastics[3,5,10]	38 ± 3 to 64 ± 2	5 × 8	SE	Piston-like; triggered by magma withdrawal of trachyte lavas and lateral dyke injection
Paka	0.92° N 36.18° E	Unknown	Trachyte and minor basaltic lavas [3,8]	10	1.5	SE	Unknown; probably associated with trachyte pyroclastics
Menengai	0.20° S 36.18° E	OC 200	Trachyte lavas and pyroclastics dominate with minor pantellertic rhyolites[3,9,11]	29	?	?	Two episodes of explosive caldera collapse, both associated with ignimbrites and ash fall deposits
		IC?		8	12 × 8	NE	Incremental; at least five phases of collapse, each represented by low-volume ignimbrites creating a scalloped caldera edge
Longonot	0.91° S 36.45° E	400	Trachyte lavas, airfall and ignimbrites with minor mixed basaltic–trachyte lavas[12,13,14]	21	12 × 8	NE	Piston-like block; magmatic overpressure from volatile exsolution, magma–water interaction and influx of magma into reservoir
Suswa	1.18° S 36.35° E	OC 100–240	Phonolite and trachyte lavas and tuffs[9,15,16,17,18]	100–240	12 × 8	ENE	Magma withdrawal at depth followed by resurgence of an 'island-block'
	–	IC?		?	5	NE	

OC, outer caldera; IC, inner caldera. References: 1, Brown & Carmichael (1971); 2, Williams *et al.* (1984); 3, Bloomer *et al.* (1989); 4, Bosworth *et al.* (2003); 5, Weaver (1977); 6, Dunkley *et al.* (1993); 7, Black *et al.* (1998); 8, Woolley (2001); 9, Macdonald (2012); 10, Smith *et al.* (1995); 11, Leat (1984); 12, Scott (1980); 13, Scott & Skilling (1999); 14, Macdonald & Scaillet (2006); 15, Baker *et al.* (1988); 16, Johnson (1969); 17, Skilling (1993); and 18, Macdonald *et al.* (1993).
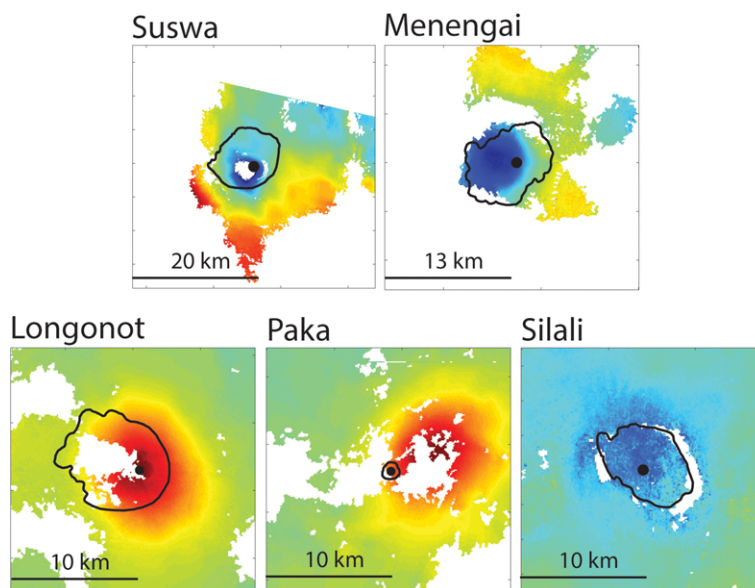
Fig. 3. Interferograms showing ground deformation at Kenyan caldera volcanoes. Subsidence (blue colours) of 2–5 cm occurred at Suswa and Menengai between 1997 and 2000. At Suswa the subsidence was confined within the caldera, whereas at Menengai the signal extends beyond the caldera boundary. The signal at Longonot shows c. 9 cm of uplift (red) between 2004 and 2007 centred east of the caldera, but on top of the recent pit crater. Uplift of c. 21 cm at Paka volcano occurred between 2006 and 2007. The signal is located NE of the crater and is seen over a large spatial distance compared with the caldera. Subsidence of c. 1.5 cm between 2007 and 2010 is centred over Silali's caldera.

published work. Trachyte and basaltic lava flows dominate in northern Kenya, whereas the southern volcanoes are almost exclusively trachytic in composition.

Extensional faulting, pyroclastic cones, fissures, off-edifice eruption centres and cinder cones are common throughout the Kenyan Rift and frequently show alignment. At Silali, Emuruangogolak and Paka, major faulting and extensive dyke intrusion has produced NNE–SSW-aligned chains of basaltic fissures and cones (Weaver 1977; Dunkley *et al.* 1993; Macdonald 2012). At Emuruangogolak, these events produced an extensive 9 km-long chain of aligned fissures north of the volcano (Dunkley *et al.* 1993; Black *et al.* 1998; Woolley 2001). However, there are few, if any, aligned faults and fissures at Suswa, the Barrier and Menengai. Longonot hosts a number of off-edifice eruption centres that are aligned parallel with intra-rift extensional faults. There are also a number of pyroclastic cones located on Longonot's flanks, but they are not located on fault scarps.

Methods

To investigate the tectonic and structural control on caldera ellipticity and orientation in Kenya, we determined the extensional setting, fault orientations and the pre-existing rift fabric direction. We used remote sensing techniques and existing geological maps to identify and measure structural features at each caldera and we calculated the azimuth of the modern day relative plate motion vector from the GPS-derived plate-kinematic model of East Africa. Data sources included the GPS-derived plate-kinematic model of East Africa, Advanced Spacebourne Thermal Emission and Reflection Radiometer (ASTER) and ASTER GDEM Version 2 Digital Elevation Model imagery, in addition to information from previously published work. Analyses of the data were performed using ENVI Version 4.8, ESRI ArcGIS Version 10.0 and MATLAB Version 7.9 R2009b software.

Calderas

The ellipticity and elongation orientation of Kenyan calderas were determined by digitizing their surface expression as a series of points in ArcGIS from ASTER imagery. Paka has a small sub-circular summit caldera that is breached by two craters extending SE and WSW. These are thought to have formed concurrently with caldera collapse and create the impression of a strongly elongated

caldera (Dunkley *et al.* 1993). Previous studies have included the extent of both craters in their analysis of elliptical calderas (Bosworth & Strecker 1997; Bosworth *et al.* 2000); however, we constrained our analysis to include only the area bounded by mapped volcanic ring faults. We believe this is justified because there is no evidence to suggest that these other features formed concurrently with caldera collapse.

We used the Standard Deviation Ellipse function within ArcGIS to calculate the best-fitting ellipse associated with each caldera and we calculated the eccentricity using the output values of the long and short axis length.

Fault populations

Rift border faults were mapped from the 1:1 000 000 Geological Map of Kenya that was compiled for the Petroleum Exploration Promotion Project (BEICIP 1987). We imported the map into ArcGIS and digitized the faults to create a polyline shape layer. Each fault was represented as a single polyline with multiple linear segments (to represent curvilinear faults); the azimuth of a fault was calculated as the non-weighted average azimuth of all linear segments. For each fault population, we calculated the mean orientation, the variance and the 95% confidence intervals. We calculated length-weighted rose diagrams for each fault population to aid visualization of the dominant orientations. We present both the calculated mean and the rose diagrams on northern hemisphere grids (i.e. $270-90°$). The mean azimuth of a fault population is shown as a solid line with unit length and the 95% confidence interval (the interval within which 95% of the population distribution of fault azimuths lie) as a solid arc. These values are superimposed on the corresponding length-weighted rose diagram. Note that, arithmetically, the largest bin on the length-weighted rose diagram, that is, the modal fault direction, is rarely the same as the calculated mean fault direction.

At each caldera, we limited the number of faults analysed by measuring an area related to the surface extent of volcanic deposits, primarily lava flows, and the width of the rift. We created a bounding box for each volcano defined as an along-rift to rift width aspect ratio of 3:1, although the length of the bounding box was truncated if it overlapped with lavas from other volcanoes. The ratio was chosen for consistency across all analyses. We used ASTER satellite imagery and ASTER GDEM Version 2 to map the intra-rift faults. L1B ASTER satellite images were used in the VNIR spectrum (bands 1, 2 and 3N) at 15 m spatial resolution. The satellite images were orthorectified within ENVI using the GDEM. Image processing techniques, such as contrast stretching, band ratios and principal component analysis, were applied to the images to aid the detection of faults and volcanic features (e.g. Rowan & Mars 2003). At Longonot, Silali and Paka volcanoes we also used the geological maps produced by Clarke *et al.* (1990) to identify faults.

Faults were identified in the Proterozoic rocks using the *Geological Map of Kenya* (BEICIP 1987). We separated the faults into two geographically distinct groups that were analysed separately, with faults in the northern rift segment forming one population and faults in the southern rift segment forming a second population (Fig. 1a).

Length-weighted rose diagrams were generated using the Rose Plot v4.0 extension for ArcGIS. We calculated rose diagrams in $10°$ bins for rift border faults and $5°$ bins for both intra-rift extensional faults and faults in the Proterozoic basement. Both the circular mean and the circular variance were calculated using the CircStat toolbox in MATLAB (Berens 2009).

Plate motion

The tectonic setting at each volcano was assessed in terms of the extensional models of Tuckwell *et al.* (1996) using the angle between the rift border faults and the plate motion vector, and the angular difference between the plate motion vector and extensional intra-rift faults (Fig. 2).

The plate motion vector was calculated at each caldera using the modern plate-kinematic model of Stamps *et al.* (2008), with the Euler pole of the Somalia plate relative to the Victoria plate (Fig. 1b). The model quantifies regional deformation throughout East Africa by jointly inverting 3.2 myr average spreading rates, GPS velocities and earthquake slip vectors. We calculated the velocity azimuthal uncertainty associated with the plate motion vector at each caldera volcano.

We assumed that the plate motion vector at the time of caldera formation was the same as the modern day vector. We believe this is a reasonable assumption because proxies for the regional least-compressive horizontal compressive stress orientation have maintained a NW−SE orientation since 600 ka (Strecker & Bosworth 1991), extension rates in northern Kenya have remained consistent over 10^1-10^6 years (Melnick *et al.* 2012) and the age of caldera formation in Kenya ranges from 8 ka to $100-240$ ka (Table 2).

Results

We present here the ellipticity and orientation values of Kenyan calderas determined from satellite imagery and geological maps (Fig. 4; Table 3). We

describe the orientation of the mapped fault populations (rift border, intra-rift and Proterozoic basement faults; Table 4) and classify the extensional regime at each caldera. These results were collated and it was determined whether the calderas were aligned with the fault populations (Fig. 5).

Calderas

Figure 4 shows the topographic outline and the best-fit ellipse for each caldera (Fig. 4a–g) and the mapped rift border and intra-rift faults, effusion centres, pyroclastic cones and fissures (Fig. 4h and Fig. 4i). Calderas at the Barrier, Silali, Paka and Menengai are excellently preserved and easy to delineate from the satellite imagery. However, the calderas at Emuruangogolak, Longonot and Suswa are only partially exposed due to the overlying volcanic deposits. Although the partial exposure may introduce an error into our best-fit ellipse and consequently our caldera orientation values, we believe the error is minor because the non-exposed caldera edges could confidently be estimated using the DEM in combination with the spatial extent and deflection of lava flows.

There is a clear contrast in the long axis orientation between the northern and southern group of volcanoes. The northern group (the Barrier, Emuruangogolak, Silali and Paka) have long axis orientations ranging between 112 and 132° (ESE to SE), whereas the southern volcanic group (Menengai, Longonot and Suswa) have ENE orientations ranging between 59 and 65° (Table 3). Caldera eccentricities range from the moderately elliptical calderas at Emuruangogolak and Silali ($e = 0.7$) to the almost-circular Paka ($e = 0.94$; Table 3). If we were to include the craters extending from Paka's summit in the best-fit ellipse calculation, then its ellipticity would be very high (c. 0.5) and Paka would become the most elliptical caldera in the Kenyan Rift.

Fault populations

From north to south, the azimuth of the rift border faults change orientation from c. 24–31° (NNE) to c. 142–171° (SSE; Fig. 5, column 1, green). Fault orientation in the Proterozoic basement also varies geographically (Fig. 5, column 3), creating two distinct populations. In northern Kenya, the Proterozoic faults have a mean orientation of 124.7 ± 17.3° and in southern Kenya they have a mean direction of 352.3°, but have a high variance of 0.92 (Table 4). The length-weighted rose diagram for the Proterozoic faults in southern Kenya displays a clear bimodal distribution, with modal orientations at c. 50° and c. 75° (Fig. 5; column 3, beige rose diagrams). Our calculations for the circular mean

assume an underlying normal distribution that clearly is not the case for the southern Proterozoic faults; therefore we use the rose diagram only to interpret these faults.

The orientations of intra-rift faults throughout the Kenyan Rift are consistent, as shown by their low variances and tight clustering in the rose diagrams (Table 4; Fig. 5, column 2, light blue rose diagrams). In northern Kenya, intra-rift faults strike between 19 and 35°; in the south they have a mean strike of 178° at Menengai, 140° at Longonot and 5° at Suswa. Within the 95 percentile error, the strike of the rift border faults and the intra-rift faults at each caldera are statistically similar (Fig. 5; column 1). However, at Suswa volcano the two fault populations are mildly oblique. This is because the intra-rift faults at Suswa volcano are part of the Magadi Fault Swarm, a high frequency of north–south-trending faults, just south of the volcano, that extends into northern Tanzania (Baker 1958, 1986; Baker & Mitchell 1976). The faults in the Magadi sector are early to mid-Pleistocene in age, older than the Suswa volcanics, with the major grid faults forming at 0.8–0.4 Ma (Baker & Mitchell 1976). A recent two-month micro-earthquake swarm in the Magadi area indicated that these faults are active, normal and parallel to the main rift trend (Ibs-von Seht *et al.* 2001).

Regional tectonics

The azimuth of the GPS plate motion vector steadily increases from 104 to 109° from north to south (Table 4). To determine the extensional setting at each caldera, in Figure 5, column 1 we plot the normal to the plate motion (yellow dashed) against the orientation of the rift border faults (green) and intra-rift faults (blue).

As rift border faults and intra-rift faults have statistically similar orientations surrounding most calderas, the extensional setting in Kenya is dominantly orthogonal or oblique. In northern Kenya, the normal to the plate motion vector aligns with both the rift border and intra-rift faults, indicating orthogonal extension, although Emuruangogolak has a small angular difference that indicates mild obliquity. At Longonot, in southern Kenya, the normal to the plate motion vector is clearly oblique to both the rift border and intra-rift fault orientations, with an angular difference of c. 32°. Therefore, Longonot is in oblique extension. At Suswa, the normal to the plate motion vector is also oblique to both fault populations at c. 13° angular difference. However, the presence of the Magadi Fault Swarm results in a small statistical angular difference between the orientations of the intra-rift and rift border faults. Therefore, Suswa is considered as being in transtension. Menengai is
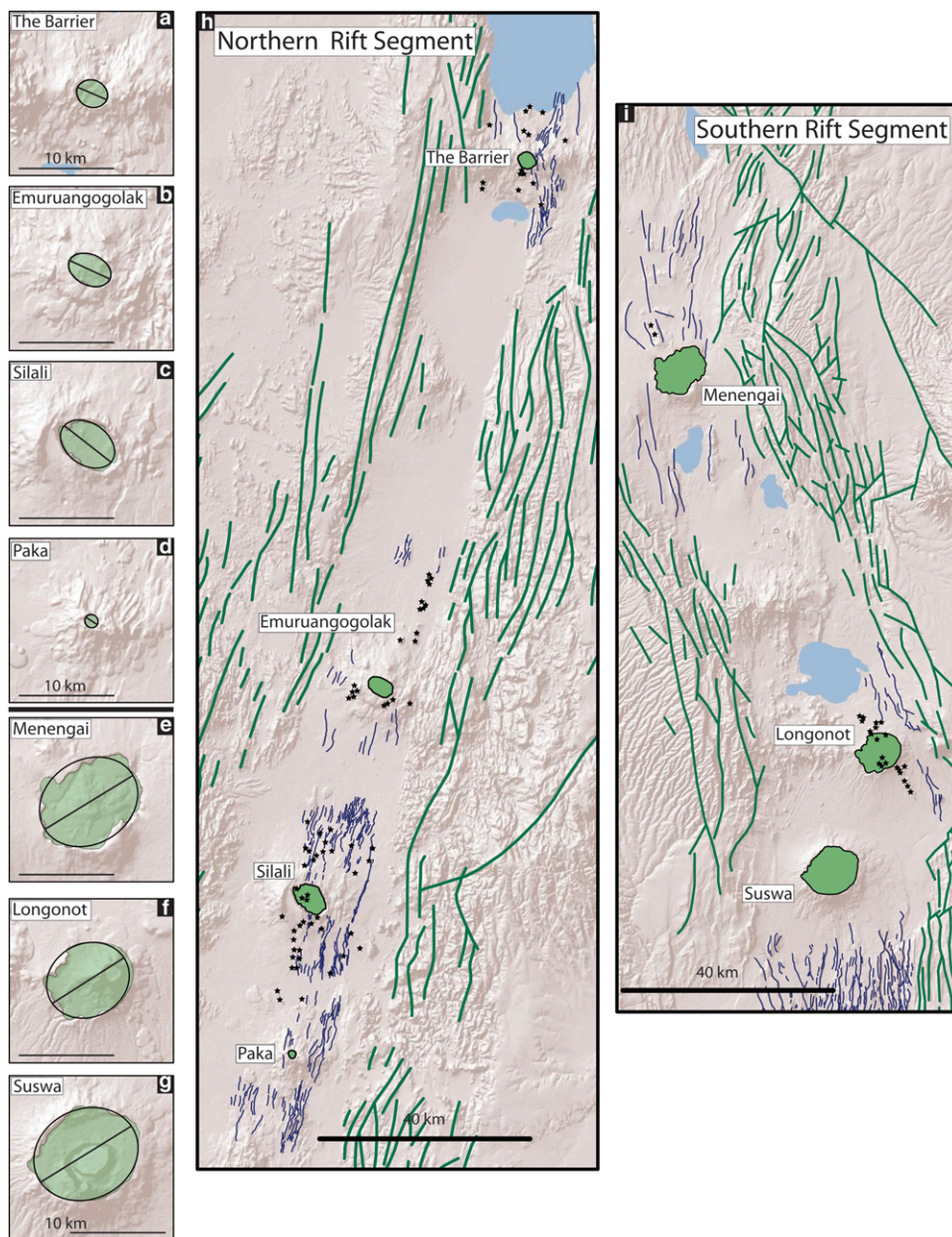
Fig. 4. Digitized topographic expression of Kenyan Rift calderas (**a–g**; green infill) and their corresponding best-fit ellipses (black ellipses). (**h, i**) Relationship between rift border faults (green), intra-rift faults (blue), volcanic features (e.g. pyroclastic cones and fissures; black stars) and calderas for the northern and southern Kenyan Rift segments. Note that only intra-rift faults surrounding caldera volcanoes are mapped.

situated roughly at the Equator where the rift border faults rotate from NNE–SSW to NNW–SSE (Fig. 5, column 2). Consequently, Menengai sits in an extensional setting that is both oblique and orthogonal.

Alignment of caldera orientation with fault populations

We tested whether the caldera short and long axes aligned with the plate motion vector, rift border or

Table 3. *Calculated plate motion vector, caldera orientation and caldera eccentricity at each Kenyan volcano*

Volcano	Plate motion azimuth		Caldera orientation	Eccentricity *e*
	°	σv_θ		
The Barrier	104.4	9.8	112.8	0.86
Emuruangogolak	104.3	10.5	115.0	0.7
Silali	104.2	10.8	124.8	0.7
Paka	104.3	11.1	132.2	0.94
Menengai	105.3	12.4	58.9	0.74
Longonot	108.8	13.6	62.6	0.86
Suswa	108.7	14	65.5	0.84

The plate motion vector and associated azimuthal error of the Somalian plate is calculated relative to the Victoria plate. Caldera orientation describes the orientation of the best-fitting ellipse of the mapped caldera and the eccentricity is also calculated from the major and minor axes of the best-fitting ellipse.

intra-rift fault orientations at each volcano (Fig. 5, column 2). As the strikes of rift border faults and intra-rift faults surrounding the calderas were statistically aligned (with the exception of Suswa), we discuss only the orientation of the intra-rift faults. No caldera has its long or short axis (red) aligned with the plate motion vector (orange). The caldera short axes align with the intra-rift faults at the Barrier and Emuruangogolak in northern Kenya, as well as Longonot in southern Kenya; at Silali and Paka the caldera short axes are misaligned with the intra-rift faults by only *c.* 1°. At Menengai and Suswa, however, the caldera short axis is misaligned by *c.* 30°. We note that, at Longonot, a series of north–south-trending intra-rift faults are located within the Olkaria Volcanic complex. These were not included in the analysis for Longonot as they are within a separate volcanic complex. However, if they were, the caldera short axis would not be parallel to the intra-rift faults, similar to Menengai and Suswa.

We also assessed the extent to which the caldera axes were aligned with Proterozoic faults. The volcanoes Barrier, Emuruangogolak, Silali and Paka are associated with the northern population of faults in the Proterozoic basement, whereas the Menengai, Longonot and Suswa volcanoes are adjacent to the southern group of Proterozoic rocks. Figure 5, column 3, shows that all the caldera long axes are aligned with the Proterozoic faults. In the northern segment, the angular difference between these faults and the caldera long axes is negligible at Silali, at *c.* 12° for the Barrier and Emuruangogolak and at 7° for Paka; all are, however, statistically aligned within error. The Proterozoic faults in southern Kenya are more variable than in northern Kenya and clearly show a bimodal

distribution with dominant populations at *c.* 45° and *c.* 77°. The caldera long axes for the southern group of volcanoes are situated between 59 and 69° and therefore lie within the bimodal Proterozoic fault population.

Discussion

The Kenyan Rift can be separated into two distinct segments: a northern rift segment that extends from the Equator towards Ethiopia and has a NNE–SSW orientation; and a southern segment that extends towards Tanzania and has a SSE–NNW orientation (Fig. 1).

In northern Kenya, the Barrier, Silali and Paka volcanoes are in orthogonal extension, as intra-rift faults and rift border faults are statistically aligned and are orthogonal to the plate motion vector. Therefore, these volcanoes are in orthogonal extension. At Emuruangogolak, the fault populations are a few degrees misaligned relative to the plate motion, but still reflect an orthogonal setting. Calderas in the northern segment are orientated SE–NW. Their short axes are aligned with the intra-rift faults and their long axes are aligned with the pre-rift Proterozoic faults.

In southern Kenya, intra-rift faults surrounding the volcanoes Menengai, Longonot and Suswa show general alignment with the rift border faults, but these fault populations are oblique to the plate motion vector. In general, the southern rift segment is considered to be in oblique extension, with the angle of obliquity between plate motion and faults at 30–35°. Calderas in the southern rift segment are orientated NE–SW. With the exception of Longonot, the caldera short axes at these volcanoes are oblique to the intra-rift fault
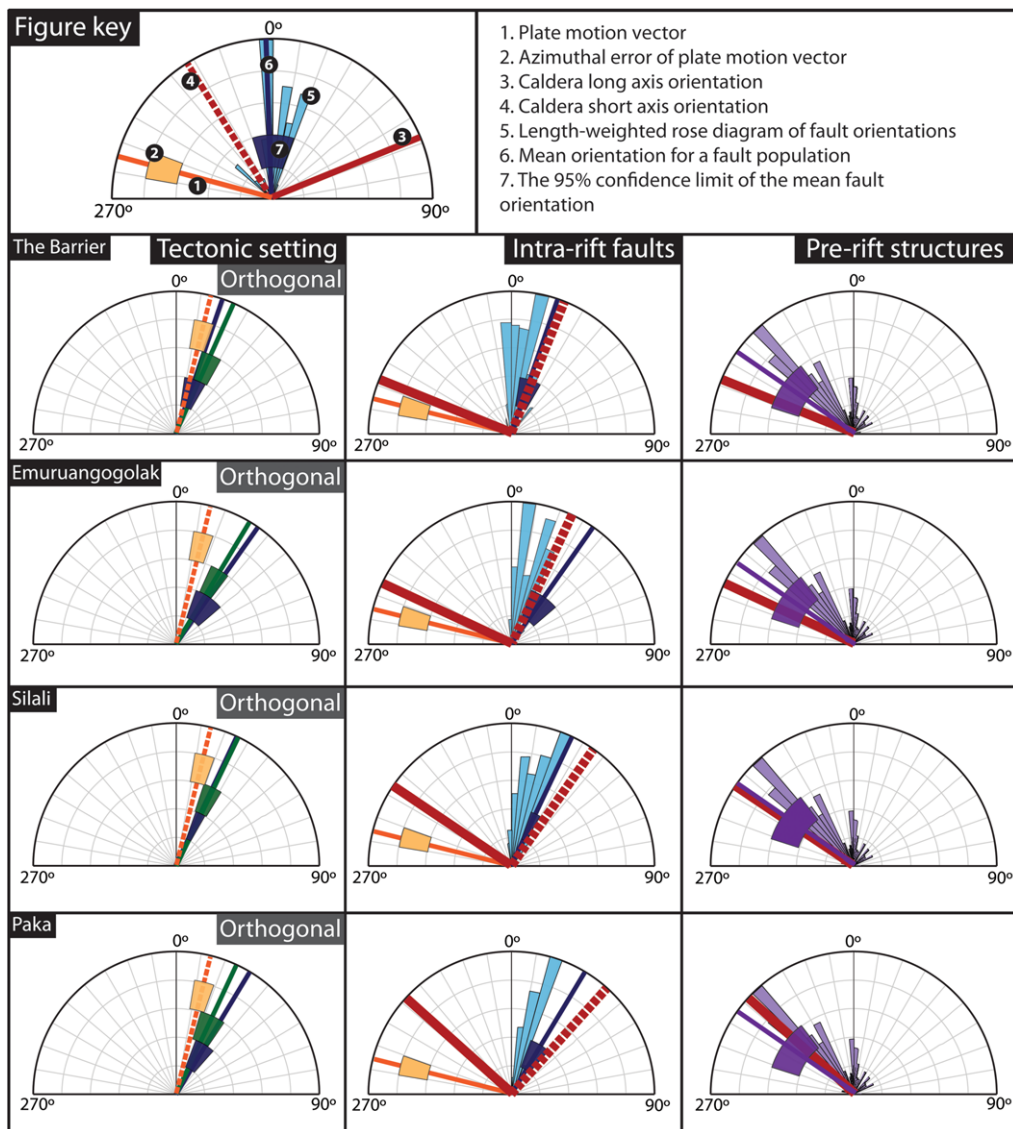
Fig. 5. Results for the extensional setting and alignment of calderas with regional stresses and pre-existing structures. **Column 1:** Extensional tectonic setting at each caldera volcano. The orientation of intra-rift faults (blue), rift border faults (green) and the normal to the plate motion vector (orange dashed) are shown with associated errors. The acute angle between each structural element is used to determine whether the setting is oblique, in transtension or under orthogonal opening. **Column 2:** Orientation of intra-rift faults with respect to caldera orientation. Intra-rift fault orientations are displayed using both length-weighted rose diagrams (light blue) and the frequency-weighted circular mean orientations (dark blue). Caldera long axis orientations are shown in red and short axis orientations are dashed. **Column 3:** Orientation of Proterozoic faults with respect to caldera long axis orientation. Faults mapped in the Cherangani Hills are shown as a purple length-weighted rose diagram and the frequency-weighted circular mean orientation is marked in dark purple. In a similar fashion, faults mapped in Loita Hills are presented in beige.

orientations. However, at all three volcanoes, the caldera long axes are aligned with the Proterozoic fault orientation.

Our results, therefore, show that these two rift segments are different in their tectonic and caldera characteristics. The contrast between these two rift
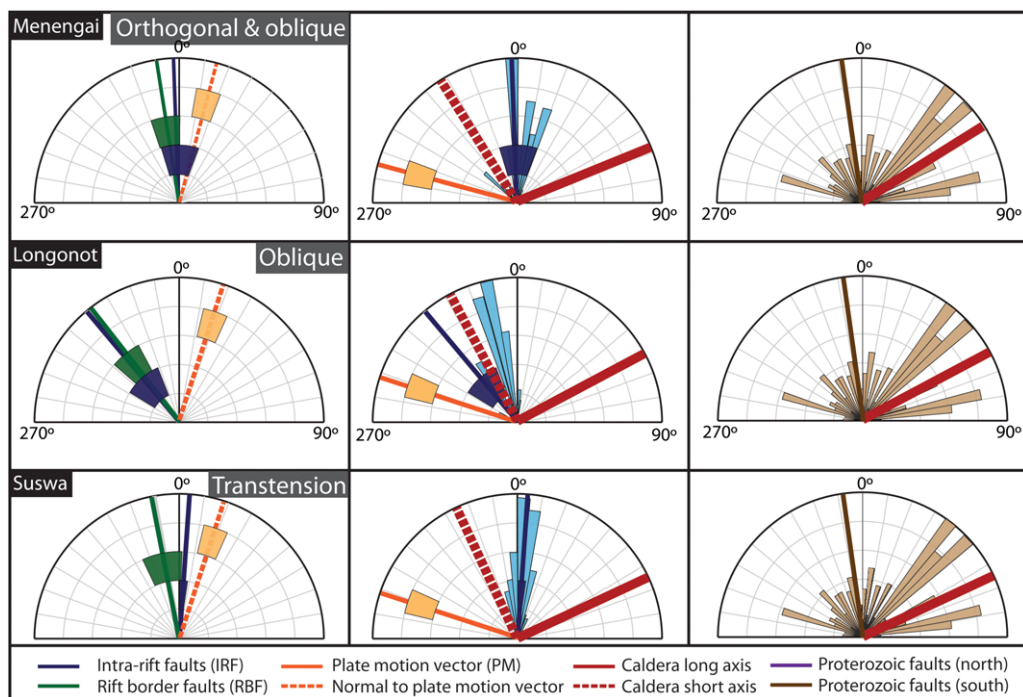
Fig. 5. *Continued.*

segments allows us to investigate the role of extensional settings in caldera orientation.

Caldera eccentricity and orientation

Our remote sensing results show that all seven Kenyan calderas are elliptical. We found no trend in ellipticity between the two rift segments, nor was there any trend between ellipticity, age, caldera size or eruptive volume. Over half of all calderas globally are elliptical, with short/long axis ratios <0.95 (Fig. 6; Geyer & Martí 2008); a third of all calderas have ellipticity values between 0.65 and 0.84, similar to those of the Kenyan calderas (Table 3). The range of values from Kenya coincides with values from the MER and the Taupo Volcanic Zone (New Zealand), both continental rift zones. Figure 6 shows that there are few calderas worldwide with ellipticity values between 0.85 and 0.94; we suggest this is a dataset artefact because equal short and long axis lengths are more likely to be recorded at near-circular calderas. For example, from our analysis, the Barrier, Paka and Longonot calderas have ellipticity values between 0.85 and 0.9 as a consequence of our ellipse-fitting technique, but in the Collapse Caldera Database (Geyer & Martí 2008) both Paka and Longonot are assigned to the top >0.94 bin.

Within Kenya, the caldera orientation is controlled by either the local stress field or by preexisting structures. We tested these hypotheses by comparing caldera orientation with our measured proxy stress field and mapped the pre-existing structures. We did not observe strike-slip faults in our analysis of intra-rift faults, therefore we assumed that all the intra-rift faults were normal and used their orientation as a proxy for the horizontal stress field. However, the exact horizontal stress field orientation is notoriously difficult to measure (e.g. Zoback *et al.* 1987; Arnold & Townend 2007; Delvaux & Barth 2010). None the less, intra-rift faults surrounding each caldera have consistent orientations with low variances (Table 4) and so we assumed that they all formed under uniform stress with a consistent orientation, which we termed the horizontal tensile stress orientation.

Aligned volcanic features, such as effusion centres and pyroclastic cones, can indicate the orientation of shallow crustal stresses. Figure 4 shows the mapped locations of pyroclastic cones, off-edifice point effusion centres and fissure vents (black stars). Although we could not statistically determine their alignment, it was clear that they also followed the trend of intra-rift faults, particularly at Emuruangogolak, Silali and Longonot. At Longonot, intra-rift faults (aligned with the rift border faults)
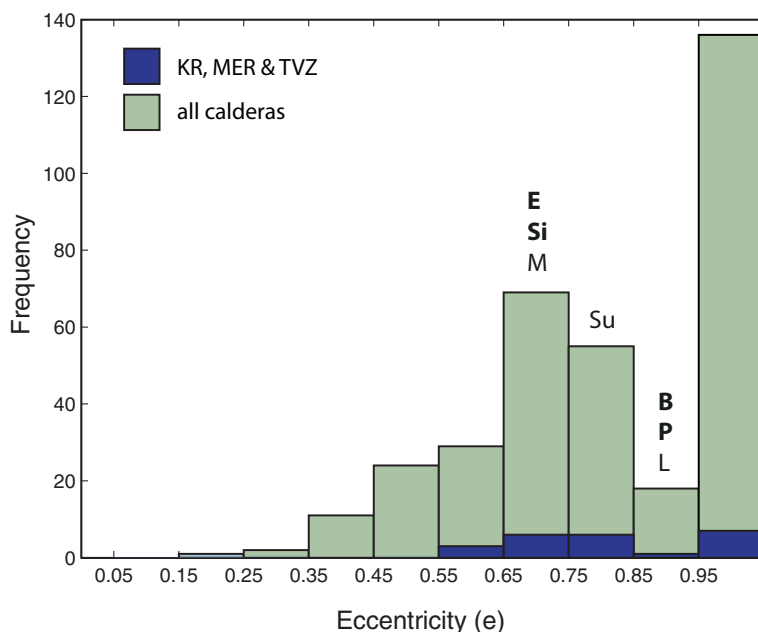
Fig. 6. Eccentricity of calderas worldwide, data extracted from the Collapse Caldera Database (Geyer & Martí 2008). Eccentricity of calderas in the Kenyan Rift (KR), Main Ethiopian Rift (MER) and the Taupo Volcanic Zone (TVZ) are shown in the darker shade. The eccentricity of Kenyan calderas, calculated in this study, are marked above the histogram bars. B, the Barrier; E, Emuruangogolak; Si, Silali; P, Paka; M, Menengai; L, Longonot; and Su, Suswa.

offset early Pleistocene–Pliocene trachytes, but only a few faults offset later mid–late Pleistocene–Holocene trachytes NE and SE of the edifice (Clarke *et al.* 1990). This indicates that these faults formed contemporaneously with periods of volcanism. We therefore assumed that the volcanic features and extensional intra-rift faults formed under the same crustal stresses.

In northern Kenya, the caldera long axes are perpendicular to the intra-rift faults. The caldera long axes are also statistically parallel to the NW–SE-trending Proterozoic faults, which are thought to underlie the Kenyan Rift (Mosley 1993). Assuming that the caldera geometry is a proxy for the magma reservoir geometry, our results show that two processes could control the caldera orientation in the northern Kenya. First, horizontal compressive stresses may cause a magma reservoir to form perpendicular to the minimum stress (Table 1, 1a). Alternatively, the magma storage region may align with the pre-existing NW–SE fault network (Table 1, 1c). This picture, however, may

Table 4. *Results from the structural measurements of faults determined from remote sensing*

Volcano	Intra-rift faults				Rift border faults				Proterozoic faults			
	Mean	σ^2	Range	N	Mean	σ^2	Range	N	Mean	σ^2	Range	N
The Barrier	19.2	0.14	22.6	43	24.8	0.07	12.5	52	124.7	0.57	34.6	43
Emuruangogolak	35.0	0.12	29.3	25	31.4	0.10	13.2	69	124.7	0.57	34.6	43
Silali	25.9	0.21	12.1	192	25.8	0.26	17.0	118	124.7	0.57	34.6	43
Paka	31.1	0.26	21.4	75	25.8	0.26	17.0	118	124.7	0.57	34.6	43
Menengai	178.5	0.27	34.1	31	171.4	0.39	18.7	162	352.3	0.92	—	25
Longonot	140.3	0.24	37.6	24	142.0	0.32	20.7	101	352.3	0.92	—	25
Suswa	4.8	0.13	8.6	276	169.3	0.34	27.6	61	352.3	0.92	—	25

Mean orientation, circular variance (σ^2) and the angular range of the 95% confidence interval for fault populations is shown.

be more complex than a two end-member model, with interactions between the two processes. For instance, basement anisotropies on the eastern flanks are not parallel to recent Quaternary volcanic features (Bosworth *et al.* 2003), but joint systems may have acted as magma conduits (Key *et al.* 1989; Haug & Strecker 1995). Furthermore, rifting may have locally altered the strike of Proterozoic shear zones (Hetzel & Strecker 1994), which, in turn, may influence magma pathways and the surface expression of the resulting volcanic activity.

Calderas in the southern rift segment have long axes oblique to intra-rift faults and are, therefore, not aligned with the regional horizontal stress orientation; an exception is Longonot volcano. All the calderas are, however, aligned between the bimodal orientation of the pre-rift Proterozoic fabric. We consider these calderas to be aligned with the pre-existing structures through two possible mechanisms. First, magma storage regions can consist of an interconnected series of sills (e.g. Hildreth 1981; Dawson *et al.* 2004; Sánchez *et al.* 2004). These sills may exploit either modal pre-existing fault orientation. Thus, although individual sills have varying orientations, the overall complex is elongated between these two modal orientations. Alternatively, the intersections where two sets of pre-existing faults cross are comparatively weak compared with the surrounding rock. In this case, the magma will accumulate at these intersections and along both faults. As in the first mechanism, the reservoir region will not appear to be elongated along one modal pre-existing orientation, but between them the two. Both mechanisms suggest that the orientation of elliptical calderas in the southern rift segment is controlled by the underlying pre-rift basement structure.

Extensional settings

Our results show that the volcanoes in the Kenyan Rift are situated across a variety of extensional settings, from orthogonal in the north to oblique in the south. Globally, transtension and orthogonal extensional settings are dominant and oblique extension, such as that observed in the southern Kenyan Rift segment, is unusual (Fig. 7). At Suswa, the intra-rift faults are part of the Magadi Fault Swarm, which possibly extends under the edifice. There are no intra-rift faults or volcanic alignments north of Suswa, or on Suswa itself, so our statistical analysis was based solely on the Magadi faults. If the intra-rift faults were aligned with the rift border faults under Suswa, as seen at the other volcanoes, Suswa would also be considered oblique. Menengai volcano has components of both orthogonal and oblique extension. This is due to the en echelon change in orientation of the rift border faults

surrounding the caldera – a consequence of Menengai being situated at the junction between the northern and southern rift segments.

As a result of the complexity in the fault patterns in the MER, studies of rift kinematics in this region often define extension in terms of orthogonal, low/moderate obliquity ($\alpha \leq 45°$) and high obliquity ($\alpha \leq 45°$; e.g. Agostini *et al.* 2009; Corti 2012). If we were to use this definition, the volcanoes in the northern rift segment would remain classified as orthogonal, with the exception of Emuruangogolak, which would be classified as low obliquity. All the volcanoes in the southern rift segment would also be classified as low obliquity.

We can compare structural and magmatic factors such as the spreading rate, magma supply rate and crustal thickness of the southern Kenya Rift with the transtensional MER to ascertain why we observe the unusual case of oblique rifting. The MER, also in the EARS, is a comparable extensional setting as it consists of a 60–85 km wide fault-bounded valley and contains extensional intra-rift faults, basaltic fissures and silicic caldera volcanoes (e.g. Corti 2009). Here the extension rate is *c.* 6 mm a^{-1} and the strain is accommodated along narrow (20 km) localized magmatic segments that are oblique to the boundary faults (Ebinger & Casey 2001; Mackenzie *et al.* 2005; Maguire *et al.* 2006). It is thought that this rift obliquity has controlled the evolution and segmentation of the MER (Corti 2008). The crustal thickness varies from 30 to 35 km in the northern sector to *c.* 35–40 km in the central sector (Maguire *et al.* 2006). Using values reported in Bendick *et al.* (2006), the MER calderas are situated in a transtensional setting (Fig. 7), one of the dominant extensional regimes globally. The plate motion vector has remained constant over the past 11 myr (Royer *et al.* 2006) and so it is the shift in strain accommodation from the rift border faults to oblique intra-rift faults that classifies the MER as transtensional.

In the Kenyan Rift, the change from orthogonal to oblique extension is reflected by the change in the rift border fault orientation with respect to the plate motion vector. During the evolution of a continental rift, mechanical processes largely control rift segmentation, as well as the contribution of asthenospheric processes such as upwelling, so a combination of both these processes may be controlling the Kenyan Rift segments (Ebinger & Casey 2001; Casey *et al.* 2006). Alternatively, and our preferred explanation, pre-existing basement anisotropies could have been reactivated during extension and guided rift border fault orientation in this rift segment. The presence of NW–SE shear zones in Proterozoic rocks has influenced at least the initial evolution of the Kenyan Rift.
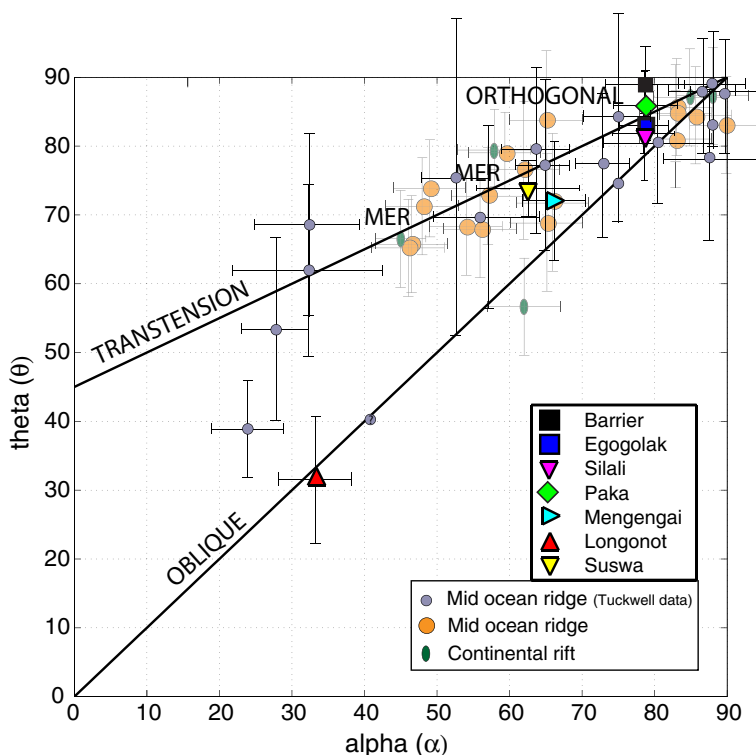
Fig. 7. Plot of the acute angle θ between relative plate motion and extensional fault orientation versus the acute angle α between the relative plate motion vector and the trend of the plate margin (or rift border faults). Locations in oblique opening plot along $\theta = \alpha$, transtensional settings lie on $\theta = 45° + \alpha/2$ and orthogonal opening clusters around $\theta = \alpha = 90°$. Results from our Kenyan analysis are plotted individually as squares and isolated results from volcanoes in the Main Ethiopian Rift (MER) are labelled – the MER results are not representative of the whole rift, as the faults in general have highly variable orientations (Corti 2012). Data from Tuckwell *et al.* (1996) are from mid-ocean ridge settings. Data extracted from Rowland & Sibson (2001), Acocella *et al.* (2002, 2003), and Bendick *et al.* (2006).

The spreading rate and rift maturity also affect continental rift structure (Ebinger 2005). At MORs, Tuckwell *et al.* (1996) have suggested that slow-spreading MOR settings (half-rate <20 mm a^{-1}) tend to be in transtension and fast-spreading ridges tend to spread orthogonally. However, as MOR settings are the end-member of the entire rifting process and extension rates at continental rifts are extremely slow (Kenya Rift, *c.* 3–4 mm a^{-1}; MER, *c.* 6 mm a^{-1}), comparison between these two settings is perhaps not appropriate. Assuming that the spreading rate reflects the magma supply rate, we would not expect major differences in the magma supply rate between the Kenya Rift and the MER. Thus, these two rifts cannot be characterized by major differences in their magma supply rates. The mechanical strength of the lithosphere is controlled by its thickness, which influences the structure of a rift (e.g. a wide or narrow rift; Buck 2004). Crustal thickness in the oblique southern

Kenyan Rift is 35 km, broadly similar to the MER crustal thickness at 30–40 km (Prodehl *et al.* 1997; Stuart *et al.* 2006). Therefore, we cannot distinguish between these two rifts based on crustal thickness alone.

Magma rise in oblique extensional settings

Our results show that the northern rift segment in Kenya is in orthogonal extension and is characterized by elliptical calderas that are parallel to both the minimum horizontal stress orientation and Proterozoic pre-existing structures. Therefore, we were unable distinguish which process controls caldera orientation in northern Kenya. The southern rift segment is in oblique extension and calderas in this section are orientated along pre-existing structures. Thus, we conclude that, in the oblique section of the Kenyan Rift, pre-existing structures play

a dominant role in magma reservoir development and the rise of magma through the lithosphere.

The influence of pre-existing structures on rift architecture and volcanism has been suggested elsewhere in the EARS (Morley *et al.* 1992; Ring 1994; Korme *et al.* 2004). For example, within the MER, pre-rift east–west structures appear to control the orientation of some elliptical calderas at Gariboldi, Gedemsa and Fantale volcanoes (Acocella *et al.* 2003). Pre-existing structures can control magma rise in the crust in a number of ways (Acocella *et al.* 2003): (a) the sub-vertical attitude of crustal-scale pre-existing structures may allow easy magma intrusion; (b) the reactivated fault networks may create localized areas of extension, such as releasing bends or pull-apart structures, which focus the rise of magma; and (c) pre-existing structures are deeper than the recent rift-related faults and, therefore, affect magma accumulation in the mid-crust. We propose that magma rise in the oblique Kenyan Rift is also controlled by one or more of these processes.

In the Tanzanian Divergence, just south of the Kenyan Rift, Isola *et al.* (2014) showed that heterogeneity in the strain field controls the rise of magma across different rift segments. Specifically, they identified that pre-existing rift structures have a greater influence on the orientation of volcanic features than more mature rift segments. This is probably due to thermo-mechanical modifications in mature segments allowing the tectono-magmatic system to directly respond to regional crustal stresses (i.e. stresses associated with the extension direction). This hypothesis broadly agrees with our results, as we have shown that magma reservoirs in the less mature southern rift segment are influenced by pre-existing structures. We cannot test this hypothesis for the northern rift segment as the calderas align to both pre-existing structures and the regional stress field. However, if this mechanism were to apply to the Kenyan Rift, we would infer that the magma reservoir geometry for the northern calderas is controlled by the regional crustal stresses.

Structural control of magmatism at different crustal levels

Volcanic features, such as pyroclastic cones and effusive vents, are typically aligned with extensional intra-rift faults. The two main models used to explain fault and volcanic alignments are fracture-induced extension and dyke-induced fracturing (e.g. Acocella *et al.* 2003; Tentler 2005). In the fracture-induced model, fractures and fissures propagate downwards through the crust from the Earth's surface. When they reach the tensile limit of the lithosphere, the fractures become normal

faults and are unlikely to reach depths greater than 2 km (Acocella *et al.* 2003). The formation of fracture-induced normal faults does not require the initial presence of magma or a dyke intrusion within the crust. Based on this model, these open faults or fractures act as conduits for the rise of magma and eruption along fissure vents (Chorowicz *et al.* 1994; Korme *et al.* 1997, 2004). In the dyke-induced model, magma is intruded into the crust and forms a magmatic plumbing system that feeds dykes and aligned volcanic features (Rooney *et al.* 2011). Surface faulting is induced by the tensile stresses as a result of dyke emplacement and magma rise consequently follows (Rowland *et al.* 2007). Thus, both dykes and faults in this model originate within the crust and propagate towards the Earth's surface.
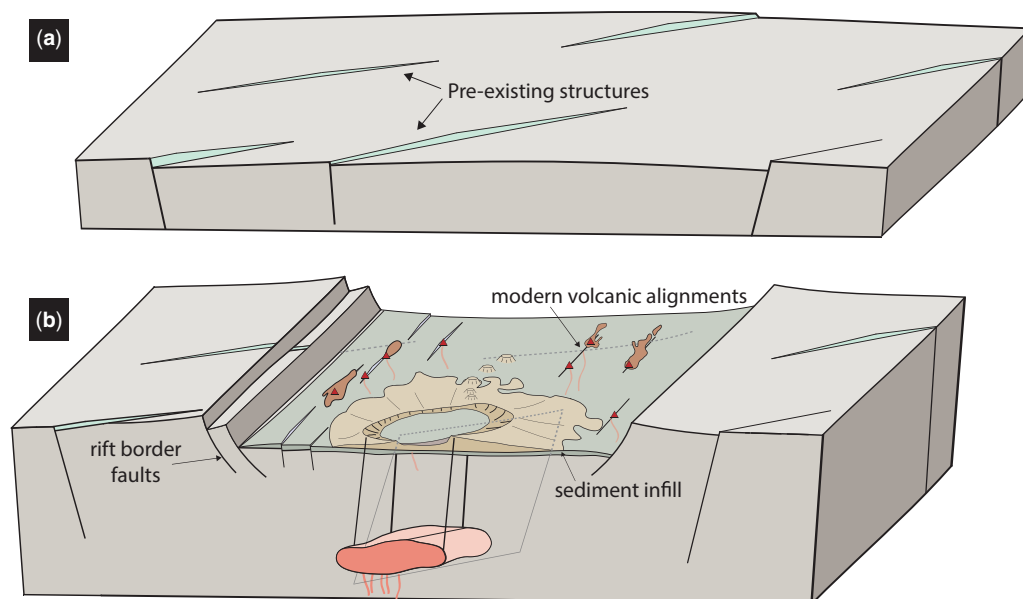
In the oblique southern Kenyan Rift, aligned intra-rift faults and volcanic features are oblique to the caldera orientation and our inferred magma reservoir orientation. Assuming that the intra-rift faults are shallow (*c.* 2 km) and that the magma reservoirs are deeper, different lithospheric stresses must be acting separately on the faults and the magma reservoirs. From this perspective, it seems likely that the pre-existing Proterozoic structures could control the orientation of magma reservoirs, but not the intra-rift fault orientation (Fig. 8). Consequently, we suggest that intra-rift faults and aligned volcanic features develop through fracture-induced extension because this model does not require a magmatic plumbing system to induce fault formation.

Oblique extension and volcanism

Our results provide a broad prospective on the observed changes in magma composition throughout the Kenyan Rift. In the northern rift segment the eruptive products are bimodal, typically trachyte pyroclastics and trachyte/basaltic lavas. In southern Kenya, the eruptive products are almost entirely trachytic, but are also compositionally zoned. This observation led Macdonald (2012) to propose significant periods of quiescence and stability within the southern mafic systems, sufficient to allow substantial magma evolution. We speculatively suggest that the oblique structures, which control magma rise in the southern rift segment, may cause the magmas to stall in the upper crust, thereby creating the time required to develop compositional zoning.

Caldera systems are assumed to reflect the geometry of past magma reservoirs. Geophysical observations, such as interferometric synthetic aperture radar (InSAR), magnetotellurics and seismicity, allowed us to conduct a similar analysis on present magma storage. Recent InSAR observations show uplift at Paka and Longonot and subsidence at

Fig. 8. Summary model for magma storage in the southern Kenyan Rift. (**a**) Aligned Proterozoic faults formed prior to the Kenyan Rift. (**b**) Formation of the Kenyan Rift and onset of magmatism and the development of silicic magma reservoirs. Pre-existing Proterozoic faults are exposed on the rift flanks, but are covered by volcanics and sediments within the rift. Rift border faults and extensional intra-rift faults form at an oblique angle to the pre-existing Proterozoic faults. Intra-rift faults form through fracture-induced extension, reaching depths less than about 2 km. Intra-rift faults act as a conduit for shallow magma rise. Silicic magma reservoirs form at depths greater than 2 km and align parallel to the underlying Proterozoic fault fabric, thus they become elliptical in plan view. During caldera-forming eruptions, the geometry of the magma reservoir determines caldera ellipticity and orientation.

Suswa, Menengai and Silali (Fig. 3; Biggs *et al.* 2009, 2013). Subsidence at Silali, Menengai and Suswa is located over the calderas and may be explained by magma movement; however, processes such as cooling, crystallization and gas exsolution can also produce significant ground subsidence (Caricchi *et al.* 2014).

In contrast, uplift signals at both Paka and Longonot are offset from their calderas. At Paka, the signal is centred on the northeastern flank and, at Longonot, it is located to the east over a recently formed pit crater. These observations can be interpreted in several ways: (1) the signals are not from a potential caldera-forming reservoir; (2) the magmatic system has migrated laterally and, if an eruption were to occur, a nested caldera structure could form; and (3) the deformation may not be magmatic, but hydrothermal expansion and contraction.

Conclusion

We used remote sensing data to investigate the extensional characteristics of the Kenyan Rift and to test whether the orientation of elliptical calderas is controlled by regional stresses or pre-existing structures. Our results showed that extension in the northern Kenyan Rift is orthogonal, whereas in the southern Kenya Rift it is oblique. In northern Kenya, our analysis showed that caldera orientation can be explained by either regional stresses or pre-existing structures, but that only pre-existing structures control caldera orientation in the southern rift segment.

Our results highlight the role of different structures on magma rise at different crustal levels in oblique rifts. We propose that in the oblique southern Kenyan Rift, deep-seated pre-existing structures control magma rise in the lithosphere and the development of magma reservoirs. In contrast, intra-rift faults and volcanic alignments are controlled by local shallow crustal stresses due to extension. Pre-existing structures may control caldera orientation in parts of the transtensional MER and, therefore, we may expect to find that these structures control magma rise in other oblique and transtensional rifts, such as the Taupo Volcanic Zone, New Zealand.

References

ACHAUER, U. 1992. A study of the Kenya rift using delay-time tomography analysis and gravity modelling. *Tectonophysics*, **209**, 197–207.

ACHAUER, U. & MASSON, F. 2002. Seismic tomography of continental rifts revisited: from relative to absolute heterogeneities. *Tectonophysics*, **358**, 17–37.

ACHAUER, U. & KRISP TELESEISMIC WORKING GROUP 1994. New ideas on the Kenya rift based on the inversion of the combined dataset of the 1985 and 1989/90 seismic tomography experiments. *Tectonophysics*, **236**, 305–329.

ACOCELLA, V., KORME, T., SALVINI, F. & FUNICIELLO, R. 2002. Elliptical calderas in the Ethiopian Rift: control of pre-existing structures. *Journal of Volcanology and Geothermal Research*, **119**, 189–203.

ACOCELLA, V., KORME, T. & SALVINI, F. 2003. Formation of normal faults along the axial zone of the Ethiopian Rift. *Journal of Structural Geology*, **25**, 503–513.

AGOSTINI, A., CORTI, G., ZEOLI, A. & MULUGETA, G. 2009. Evolution, pattern, and partitioning of deformation during oblique continental rifting: inferences from lithospheric-scale centrifuge models. *Geochemistry, Geophysics, Geosystems*, **10**, Q11015.

AGOSTINI, A., BONINI, M., CORTI, G., SANI, F. & MAZZARINI, F. 2011. Fault architecture in the Main Ethiopian Rift and comparison with experimental models: implications for rift evolution and Nubia–Somalia kinematics. *Earth and Planetary Science Letters*, **301**, 479–492.

ARNOLD, R. & TOWNEND, J. 2007. A Bayesian approach to estimating tectonic stress from seismological data. *Geophysical Journal International*, **170**, 1336–1356.

BAKER, B. H. 1958. *Geology of the Magadi Area: Degree Sheet 51 SW Quarter. Survey, Mineralogical*. Colony and Protectorate of Kenya.

BAKER, B. H. 1986. Tectonics and volcanism of the southern Kenya Rift Valley and its influence on rift sedimentation. *In*: FROSTICK, L. E., RENAUT, R. W., REID, I. & TIERCELIN, J. J. (eds) *Sedimentation in the African Rifts*. Geological Society, London, Special Publications, **25**, 45–57, http://doi.org/10.1144/GSL.SP.1986.025.01.05

BAKER, B. & MITCHELL, J. 1976. Volcanic stratigraphy and geochronology of the Kedong–Olorgesailie area and the evolution of the South Kenya Rift valley. *Journal of the Geological Society, London*, **132**, 467–484, http://doi.org/10.1144/gsjgs.132.5.0467

BAKER, B. H. & WOHLENBERG, J. 1971. Structure and evolution of the Kenya Rift Valley. *Nature*, **229**, 538–542.

BAKER, B. H., MOHR, P. A. & WILLIAMS, L. A. J. 1972. *Geology of the Eastern Rift System of Africa*. Geological Society of America Special Papers, **136**.

BAKER, B., MITCHELL, J. & WILLIAMS, L. 1988. Stratigraphy, geochronology and volcano-tectonic evolution of the Kedong–Naivasha–Kinangop region, Gregory Rift Valley, Kenya. *Journal of the Geological Society, London*, **145**, 107–116, http://doi.org/10.1144/gsjgs.145.1.0107

BASTOW, I., NYBLADE, A., STUART, G., ROONEY, T. & BENOIT, M. 2008. Upper mantle seismic structure beneath the Ethiopian hot spot: rifting at the edge of the African low-velocity anomaly. *Geochemistry, Geophysics, Geosystems*, **9**, Q12022.

BEICIP 1987. *Geological Map of Kenya. Petroleum Exploration Promotion Project, World Bank Assistance*. Ministry of Energy and Regional Development, Nairobi.

BELLIER, O. & SÉBRIER, M. 1994. Relationship between tectonism and volcanism along the Great Sumatran fault zone deduced by SPOT image analyses. *Tectonophysics*, **233**, 215–231.

BENDICK, R., MCCLUSKY, S., BILHAM, R., ASFAW, L. & KLEMPERER, S. 2006. Distributed Nubia–Somalia relative motion and dike intrusion in the Main Ethiopian Rift. *Geophysical Journal International*, **165**, 303–310.

BERENS, P. 2009. CircStat: a MATLAB toolbox for circular statistics. *Journal of Statistical Software*, **31**, 1–21.

BIGGS, J., ANTHONY, E. Y. & EBINGER, C. J. 2009. Multiple inflation and deflation events at Kenyan volcanoes, East African Rift. *Geology*, **37**, 979–982.

BIGGS, J., ROBERTSON, E. & MACE, M. 2013. ISMER–active magmatic processes in the East African Rift: a satellite radar perspective. *In*: FERNÁNDEZ-PRIETO, D. & SABIA, R. (eds) *Remote Sensing Advances for Earth System Science*. Springer, Berlin, 81–91.

BIRT, C., MAGUIRE, P., KHAN, M., THYBO, H., KELLER, G. & PATEL, J. 1997. The influence of pre-existing structures on the evolution of the southern Kenya Rift Valley–evidence from seismic and gravity studies. *Tectonophysics*, **278**, 211–242.

BLACK, S., MACDONALD, R., BARREIRO, B. A., DUNKLEY, P. N. & SMITH, M. 1998. Open system alkaline magmatism in northern Kenya: evidence from U-series disequilibria and radiogenic isotopes. *Contributions to Mineralogy and Petrology*, **131**, 364–378.

BLOOMER, S. H., CURTIS, P. C. & KARSON, J. A. 1989. Geochemical variation of Quaternary basaltic volcanics in the Turkana Rift, northern Kenya. *Journal of African Earth Sciences*, **8**, 511–532.

BOSWORTH, W. & STRECKER, M. R. 1997. Stress field changes in the Afro-Arabian rift system during the Miocene to Recent period. *Tectonophysics*, **278**, 47–62.

BOSWORTH, W., BURKE, K. & STRECKER, M. 2000. Magma chamber elongation as an indicator of intraplate stress field orientation: borehole breakout mechanism and examples from the Late Pleistocene to Recent Kenya Rift Valley. *In*: JESSELL, M. & URAI, J. (eds) *Stress, Strain and Structure, a volume in honour of Win D. Means. Journal of the Virtual Explorer*, **2**, http://doi.org/10.3809/jvirtex.2000.00008

Bosworth, W., Burke, K. & Strecker, M. 2003. Effect of stress fields on magma chamber stability and the formation of collapse calderas. *Tectonics*, **22**, 1042.

Braile, L., Keller, G., Wendlandt, R., Morgan, P. & Khan, M. 1995. The East African Rift system. *In*: Olsen, K. H. (ed.) *Continental Rifts: Evolution, Structure, Tectonics*. Developments in Geotectonics, **25**, 213–231.

Branney, M. J. 1995. Downsag and extension at calderas: new perspectives on collapse geometries from ice-melt, mining, and volcanic subsidence. *Bulletin of Volcanology*, **57**, 303–318.

Brown, F. & Carmichael, I. 1971. Quaternary volcanoes of the Lake Rudolf region: II. The lavas of North Island, South Island and the Barrier. *Lithos*, **4**, 305–323.

Buck, W. R. 2004. Consequences of asthenospheric variability on continental rifting. *In*: Karner, G. D., Taylor, B., Driscoll, N. W. & Kohlsted, D. L. (eds) *Rheology and Deformation of the Lithosphere at Continental Margins*. Columbia University Press, New York, 1–30.

Caricchi, L., Biggs, J., Annen, C. & Ebmeier, S. 2014. The influence of cooling, crystallisation and re-melting on the interpretation of geodetic signals in volcanic systems. *Earth and Planetary Science Letters*, **388**, 166–174.

Casey, M., Ebinger, C., Keir, D., Gloaguen, R. & Mohamed, F. 2006. Strain accommodation in transitional rifts: extension by magma intrusion and faulting in Ethiopian rift magmatic segments. *In*: Yirgu, G., Ebinger, C. & Maguire, P. (eds) *The Afar Volcanic Province within the East African Rift System*. Geological Society, London, Special Publications, **259**, 143–163, http://doi.org/10.1144/GSL.SP.2006.259.01.13

Chorowicz, J. 2005. The East African Rift System. *Journal of African Earth Sciences*, **43**, 379–410.

Chorowicz, J., Fournier, J. L. & Vidal, G. 1987. A model for rift development in Eastern Africa. *Geological Journal*, **22**, 495–513.

Chorowicz, J., Collet, B., Bonavia, F. F. & Korme, T. 1994. Northwest to north-northwest extension direction in the Ethiopian rift deduced from the orientation of extension structures and fault-slip analysis. *Geological Society of America Bulletin*, **106**, 1560–1570.

Clarke, M. C. G., Woodhall, D. G., Allen, D. & Darling, G. 1990. *Geology, Volcanological and Hydrological Controls on the Occurrence of Geothermal Activity in the Area Surrounding Lake Naivasha, Kenya with Coloured 1:100 000 Geological Maps*. Report for the Ministry of Energy of Kenya.

Cole, J., Milner, D. & Spinks, K. 2005. Calderas and caldera structures: a review. *Earth-Science Reviews*, **69**, 1–26.

Corti, G. 2008. Control of rift obliquity on the evolution and segmentation of the main Ethiopian rift. *Nature Geoscience*, **1**, 258–262.

Corti, G. 2009. Continental rift evolution: from rift initiation to incipient break-up in the Main Ethiopian Rift, East Africa. *Earth-Science Reviews*, **96**, 1–53.

Corti, G. 2012. Evolution and characteristics of continental rifting: analog modeling-inspired view and comparison with examples from the East African Rift System. *Tectonophysics*, **522**, 1–33.

Corti, G., Philippon, M., Sani, F., Keir, D. & Kidane, T. 2013. Re-orientation of the extension direction and pure extensional faulting at oblique rift margins: comparison between the Main Ethiopian Rift and laboratory experiments. *Terra Nova*, **25**, 396–404.

Daly, M., Chorowicz, J. & Fairhead, J. 1989. Rift basin evolution in Africa: the influence of reactivated steep basement shear zones. *In*: Cooper, M. A. & Williams, G. D. (eds) *Inversion Tectonics*. Geological Society, London, Special Publications, **44**, 309–334, http://doi.org/10.1144/GSL.SP.1989.044.01.17

Daradich, A., Mitrovica, J., Pysklywec, R., Willett, S. & Forte, A. 2003. Mantle flow, dynamic topography, and rift-flank uplift of Arabia. *Geology*, **31**, 901.

Davis, P. & Slack, P. 2002. The uppermost mantle beneath the Kenya dome and relation to melting, rifting and uplift in East Africa. *Geophysical Research Letters*, **29**, http://doi.org/10.1029/2001GL013676.

Dawson, P., Whilldin, D. & Chouet, B. 2004. Application of near real-time radial semblance to locate the shallow magmatic conduit at Kilauea Volcano, Hawaii. *Geophysical Research Letters*, **31**, http://doi.org/10.1029/2004GL021163

Delaney, P. T., Pollard, D. D., Ziony, J. I. & McKee, E. H. 1986. Field relations between dikes and joints: emplacement processes and paleostress analysis. *Journal of Geophysical Research*, **91**, 4920–4938.

Delvaux, D. & Barth, A. 2010. African stress pattern from formal inversion of focal mechanism data. *Tectonophysics*, **482**, 105–128.

Dewey, J., Holdsworth, R. & Strachan, R. 1998. Transpression and transtension zones. *In*: Holdsworth, R., Strachan, R. & Dewey, J. (eds) *Continental Transpressional and Transtensional Tectonics*. Geological Society, London, Special Publications, **135**, 1–14, http://doi.org/10.1144/GSL.SP.1998.135.01.01

Druitt, T. & Sparks, R. 1984. On the formation of calderas during ignimbrite eruptions. *Nature*, **310**, 679–681.

Dunkley, P. N., Smith, M., Allen, D. J. & Darling, W. G. 1993. *The Geothermal Activity and Geology of the Northern Sector of the Kenya Rift Valley*. Technical Report British Geological Survey Research Report SC/93/1.

Ebinger, C. 1989. Tectonic development of the western branch of the East African Rift system. *Geological Society of America Bulletin*, **101**, 885–903.

Ebinger, C. 2005. Continental break-up: the East African perspective. *Astronomy & Geophysics*, **46**, 2–16.

Ebinger, C. J. & Casey, M. 2001. Continental breakup in magmatic provinces: an Ethiopian example. *Geology*, **29**, 527–530.

Fairhead, J. & Green, C. 1989. Controls on rifting in Africa and the regional tectonic model for the Nigeria and East Niger rift basins. *Journal of African Earth Sciences*, **8**, 231–249.

Fossen, H. & Tikoff, B. 1998. Extended models of transpression and transtension, and application to tectonic settings. *In*: Holdsworth, R., Strachan, R. & Dewey, J. (eds) *Continental Transpressional*

and Transtensional Tectonics. Geological Society, London, Special Publications, **135**, 15–33, http://doi.org/10.1144/GSL.SP.1998.135.01.02

GEYER, A. & MARTÍ, J. 2008. The new worldwide collapse caldera database (CCDB): a tool for studying and understanding caldera processes. *Journal of Volcanology and Geothermal Research*, **175**, 334–354.

GEYER, A. & MARTÍ, J. 2009. Stress fields controlling the formation of nested and overlapping calderas: implications for the understanding of caldera unrest. *Journal of Volcanology and Geothermal Research*, **181**, 185–195.

GUDMUNDSSON, A. 1995. Infrastructure and mechanics of volcanic systems in Iceland. *Journal of Volcanology and Geothermal Research*, **64**, 1–22.

GUDMUNDSSON, A. 2005. The effects of layering and local stresses in composite volcanoes on dyke emplacement and volcanic hazards. *Comptes Rendus Geoscience*, **337**, 1216–1222.

GUDMUNDSSON, A. 2007. Conceptual and numerical models of ring-fault formation. *Journal of Volcanology and Geothermal Research*, **164**, 142–160.

HAUG, G. & STRECKER, M. 1995. Volcano-tectonic evolution of the Chyulu Hills and implications for the regional stress field in Kenya. *Geology*, **23**, 165–168.

HENDRIE, D., KUSZNIR, N., MORLEY, C. & EBINGER, C. 1994. Cenozoic extension in northern Kenya: a quantitative model of rift basin development in the Turkana region. *Tectonophysics*, **236**, 409–438.

HETZEL, R. & STRECKER, M. R. 1994. Late Mozambique Belt structures in western Kenya and their influence on the evolution of the Cenozoic Kenya Rift. *Journal of Structural Geology*, **16**, 189–201.

HILDRETH, W. 1981. Gradients in silicic magma chambers: implications for lithospheric magmatism. *Journal of Geophysical Research*, **86**, 10 153–10 192.

HOLOHAN, E., TROLL, V. R., WALTER, T. R., MUNN, S., McDONNELL, S. & SHIPTON, Z. 2005. Elliptical calderas in active tectonic settings: an experimental approach. *Journal of Volcanology and Geothermal Research*, **144**, 119–136.

IBS-VON SEHT, M., BLUMENSTEIN, S., WAGNER, R., HOLLNACK, D. & WOHLENBERG, J. 2001. Seismicity, seismotectonics and crustal structure of the southern Kenya Rift – new data from the Lake Magadi area. *Geophysical Journal International*, **146**, 439–453.

ISOLA, I., MAZZARINI, F., BONINI, M. & CORTI, G. 2014. Spatial variability of volcanic features in early-stage rift settings: the case of the Tanzania Divergence, East African rift system. *Terra Nova*, **26**, 461–468.

JOHNSON, R. 1969. Volcanic geology of Mount Suswa, Kenya. *Philosophical Transactions of the Royal Society of London. Series A, Mathematical and Physical Sciences*, **265**, 383–412.

KENDALL, J., PILIDOU, S., KEIR, D., BASTOW, I., STUART, G. & AYELE, A. 2006. Mantle upwellings, melt migration and the rifting of Africa: insights from seismic anisotropy. *In*: YIRGU, G., EBINGER, C. & MAGUIRE, P. (eds) *The Afar Volcanic Province within the East African Rift System*. Geological Society, London, Special Publications, **259**, 55–72, http://doi.org/10.1144/GSL.SP.2006.259.01.06

KERANEN, K. & KLEMPERER, S. 2008. Discontinuous and diachronous evolution of the Main Ethiopian Rift: implications for development of continental rifts. *Earth and Planetary Science Letters*, **265**, 96–111.

KERANEN, K. M., KLEMPERER, S. L., JULIA, J., LAWRENCE, J. F. & NYBLADE, A. A. 2009. Low lower crustal velocity across Ethiopia: is the Main Ethiopian Rift a narrow rift in a hot craton? *Geochemistry Geophysics Geosystems*, **10**, Q0AB01.

KEY, R., CHARSLEY, T., HACKMAN, B., WILKINSON, A. & RUNDLE, C. 1989. Superimposed Upper Proterozoic collision-controlled orogenies in the Mozambique orogenic belt of Kenya. *Precambrian Research*, **44**, 197–225.

KORME, T., CHOROWICZ, J., COLLET, B. & BONAVIA, F. F. 1997. Volcanic vents rooted on extension fractures and their geodynamic implications in the Ethiopian Rift. *Journal of Volcanology and Geothermal Research*, **79**, 205–222.

KORME, T., ACOCELLA, V. & ABEBE, B. 2004. The role of pre-existing structures in the origin, propagation and architecture of faults in the Main Ethiopian Rift. *Gondwana Research*, **7**, 467–479.

KURIA, Z., WOLDAI, T., VAN DER MEER, F. & BARONGO, J. 2010. Active fault segments as potential earthquake sources: inferences from integrated geophysical mapping of the Magadi fault system, southern Kenya Rift. *Journal of African Earth Sciences*, **57**, 345–359.

LATIN, D., NORRY, M. & TARZEY, R. 1993. Magmatism in the Gregory Rift, East Africa: evidence for melt generation by a plume. *Journal of Petrology*, **34**, 1007.

LEAT, P. 1984. Geological evolution of the trachytic caldera volcano Menengai, Kenya Rift Valley. *Journal of the Geological Society, London*, **141**, 1057–1069, http://doi.org/10.1144/gsjgs.141.6.1057

LIPMAN, P. W. 1984. The roots of ash flow calderas in western North America: windows into the tops of granitic batholiths. *Journal of Geophysical Research*, **89**, 8801–8841.

MACDONALD, R. 2012. Evolution of peralkaline silicic complexes: lessons from the extrusive rocks. *Lithos*, **152**, 11–22.

MACDONALD, R. & SCAILLET, B. 2006. The central Kenya peralkaline province: insights into the evolution of peralkaline salic magmas. *Lithos*, **91**, 59–73.

MACDONALD, R., KJARSGAARD, B., SKILLING, I., DAVIES, G., HAMILTON, D. & BLACK, S. 1993. Liquid immiscibility between trachyte and carbonate in ash flow tuffs from Kenya. *Contributions to Mineralogy and Petrology*, **114**, 276–287.

MACKENZIE, G. D., THYBO, H. & MAGUIRE, P. K. H. 2005. Crustal velocity structure across the Main Ethiopian Rift: results from two-dimensional wide-angle seismic modelling. *Geophysical Journal International*, **162**, 994–1006.

MAGUIRE, P. K. H., KELLER, G. R. *ET AL.* 2006. Crustal structure of the northern Main Ethiopian Rift from the EAGLE controlled-source survey; a snapshot of incipient lithospheric break-up. *In*: YIRGU, G., EBINGER, C. J. & MACGUIRE, P. K. H. (eds) *The Afar Volcanic Province within the East African Rift System*. Geological Society, London, Special Publications, **259**, 269–292, http://doi.org/10.1144/GSL.SP.2006.259.01.21

MAHOOD, G. A. & HILDRETH, W. 1986. Geology of the peralkaline volcano at Pantelleria, Strait of Sicily. *Bulletin of Volcanology*, **48**, 143–172.

MCCALL, G. 1968. The five caldera volcanoes of the Central Rift Valley, Kenya. *Proceedings of the Geological Society of London*, **1647**, 54–59.

MCCONNELL, R. 1972. Geological development of the rift system of eastern Africa. *Geological Society of America Bulletin*, **83**, 2549–2572.

MCKENZIE, D. 1978. Some remarks on the development of sedimentary basins. *Earth and Planetary Science Letters*, **40**, 25–32.

MELNICK, D., GARCIN, Y., QUINTEROS, J., STRECKER, M. R., OLAGO, D. & TIERCELIN, J.-J. 2012. Steady rifting in northern Kenya inferred from deformed Holocene lake shorelines of the Suguta and Turkana basins. *Earth and Planetary Science Letters*, **331**, 335–346.

MOOS, D. & ZOBACK, M. D. 1993. State of stress in the Long Valley caldera, California. *Geology*, **21**, 837–840.

MORLEY, C., WESCOTT, W., STONE, D., HARPER, R., WIGGER, S. & KARANJA, F. 1992. Tectonic evolution of the northern Kenyan Rift. *Journal of the Geological Society, London*, **149**, 333–348, http://doi.org/10.1144/gsjgs.149.3.0333

MOSLEY, P. 1993. Geological evolution of the late Proterozoic 'Mozambique Belt' of Kenya. *Tectonophysics*, **221**, 223–250.

MUGISHA, F., EBINGER, C., STRECKER, M. & POPE, D. 1997. Two-stage rifting in the Kenya rift: implications for half-graben models. *Tectonophysics*, **278**, 63–81.

NAKAMURA, K. 1969. Arrangement of parasitic cones as a possible key to regional stress field. *Bulletin of the Volcanological Society of Japan*, **14**, 8–20.

NAKAMURA, K. 1977. Volcanoes as possible indicators of tectonic stress orientation–principle and proposal. *Journal of Volcanology and Geothermal Research*, **2**, 1–16.

NYBLADE, A. & ROBINSON, S. 1994. The African superswell. *Geophysical Research Letters*, **21**, 765–768.

ORSI, G., DE VITA, S. & DI VITO, M. 1996. The restless, resurgent Campi Flegrei nested caldera (Italy): constraints on its evolution and configuration. *Journal of Volcanology and Geothermal Research*, **74**, 179–214.

PHILIPPON, M., WILLINGSHOFER, E., SOKOUTIS, D., CORTI, G., SANI, F., BONINI, M. & CLOETINGH, S. 2015. Slip re-orientation in oblique rifts. *Geology*, **43**, 147–150.

POINTING, A., MAGUIRE, P., KHAN, M., FRANCIS, D., SWAIN, C., SHAH, E. & GRIFFITHS, D. 1985. Seismicity of the northern part of the Kenya Rift Valley. *Journal of Geodynamics*, **3**, 23–37.

POLLARD, D. 1987. Elementary fracture mechanics applied to the structural interpretation of dykes. *In*: HALLS, H. C. & FAHRIG, W. F. (eds) *Mafic Dyke Swarms*. Geological Association of Canada, Special Papers, **34**, 5–24.

PRODEHL, C., RITTER, J. *ET AL*. 1997. The KRISP 94 lithospheric investigation of southern Kenya–the experiments and their main results. *Tectonophysics*, **278**, 121–147.

RING, U. 1994. The influence of preexisting structure on the evolution of the Cenozoic Malawi rift (East African rift system). *Tectonics*, **13**, 313–326.

RITSEMA, J., HEIJST, H. & WOODHOUSE, J. 1999. Complex shear wave velocity structure imaged beneath Africa and Iceland. *Science*, **286**, 1925.

ROONEY, T. O., BASTOW, I. D. & KEIR, D. 2011. Insights into extensional processes during magma assisted rifting: evidence from aligned scoria cones. *Journal of Volcanology and Geothermal Research*, **201**, 83–96.

ROWAN, L. & MARS, J. 2003. Lithologic mapping in the Mountain Pass, California area using advanced spaceborne thermal emission and reflection radiometer (ASTER) data. *Remote Sensing of Environment*, **84**, 350–366.

ROWLAND, J. V. & SIBSON, R. H. 2001. Extensional fault kinematics within the Taupo Volcanic Zone, New Zealand: soft-linked segmentation of a continental rift system. *New Zealand Journal of Geology and Geophysics*, **44**, 271–283.

ROWLAND, J. V., BAKER, E. *ET AL*. 2007. Fault growth at a nascent slow-spreading ridge: 2005 Dabbahu rifting episode, Afar. *Geophysical Journal International*, **171**, 1226–1246.

ROWLAND, J. V., WILSON, C. J. & GRAVLEY, D. M. 2010. Spatial and temporal variations in magma-assisted rifting, Taupo Volcanic Zone, New Zealand. *Journal of Volcanology and Geothermal Research*, **190**, 89–108.

ROYER, J. Y., GORDON, R. G. & HORNER-JOHNSON, B. C. 2006. Motion of Nubia relative to Antarctica since 11 Ma: Implications for Nubia–Somalia, Pacific–North America, and India–Eurasia motion. *Geology*, **34**, 501–504.

RUBIN, A. M. 1995. Propagation of magma-filled cracks. *Annual Review of Earth and Planetary Sciences*, **23**, 287–336.

SÁNCHEZ, J., WYSS, M. & MCNUTT, S. R. 2004. Temporal-spatial variations of stress at Redoubt volcano, Alaska, inferred from inversion of fault plane solutions. *Journal of Volcanology and Geothermal Research*, **130**, 1–30.

SCOTT, S. 1980. The geology of Longonot volcano, Central Kenya: a question of volumes. *Philosophical Transactions of the Royal Society of London. Series A, Mathematical and Physical Sciences*, **296**, 437–465.

SCOTT, S. & SKILLING, I. 1999. The role of tephrachronology in recognizing synchronous caldera-forming events at the Quaternary volcanoes Longonot and Suswa, south Kenya Rift. *In*: FIRTH, C. R., MCGUIRE, W. J. (eds) *Volcanoes in the Quaternary*. Geological Society, London, Special Publications, **161**, 47–67, http://doi.org/10.1144/GSL.SP.1999.161.01.05

SHACKLETON, R. 1984. Thin-skinned tectonics, basement control and the Variscan front. *In*: HUTTON, D. H. W. & SANDERSON, D. J. (eds) *Variscan Tectonics of the North Atlantic Region*. Geological Society, London, Special Publications, **14**, 125–129, http://doi.org/10.1144/GSL.SP.1984.014.01.12

SHACKLETON, R. & RIES, A. 1984. The relation between regionally consistent stretching lineations and plate motions. *Journal of Structural Geology*, **6**, 111–117.

SKILLING, I. 1993. Incremental caldera collapse of Suswa volcano, Gregory Rift Valley, Kenya. *Journal of the Geological Society, London*, **150**, 885–896, http://doi.org/10.1144/gsjgs.150.5.0885

SMITH, M. & MOSLEY, P. 1993. Crustal heterogeneity and basement influence on the development of the Kenya Rift, East Africa. *Tectonics*, **12**, 591–606.

SMITH, M., DUNKLEY, P., DEINO, A., WILLIAMS, L. & MCCALL, G. 1995. Geochronology, stratigraphy and structural evolution of Silali volcano, Gregory Rift, Kenya. *Journal of the Geological Society, London*, **152**, 297–310, http://doi.org/10.1144/gsjgs.152.2.0297

SMITH, R. L. & BAILEY, R. A. 1968. Resurgent cauldrons. *In*: COATS, R. R., HAY, R. L. & ANDERSON, C. A. (eds) *Studies in Volcanology*. Geological Society of America Memoirs, **116**, 613–662.

SPINKS, K. D., ACOCELLA, V., COLE, J. W. & BASSETT, K. N. 2005. Structural control of volcanism and caldera development in the transtensional Taupo Volcanic Zone, New Zealand. *Journal of Volcanology and Geothermal Research*, **144**, 7–22.

STAMPS, D., CALAIS, E., SARIA, E., HARTNADY, C., NOCQUET, J., EBINGER, C. & FERNANDES, R. 2008. A kinematic model for the East African Rift. *Geophysical Research Letters*, **35**, L05304.

STRECKER, M. & BOSWORTH, W. 1991. Quaternary stress-field changes in the Gregory Rift, Kenya. *Eos, Transactions of the AGU*, **72**, 17–22.

STRECKER, M., BLISNIUK, P. & EISBACHER, G. 1990. Rotation of extension direction in the central Kenya Rift. *Geology*, **18**, 299–302.

STUART, G. W., BASTOW, I. D. & EBINGER, C. J. 2006. Crustal structure of the northern Main Ethiopian Rift from receiver function studies. *In*: YIRGU, G., EBINGER, C. J. & MACGUIRE, P. K. H. (eds) *The Afar Volcanic Province within the East African Rift System*. Geological Society, London, Special Publications, **259**, 253–267, http://doi.org/10.1144/GSL.SP.2006.259.01.20

SUDO, Y. & KONG, L. 2001. Three-dimensional seismic velocity structure beneath Aso Volcano, Kyushu, Japan. *Bulletin of Volcanology*, **63**, 326–344.

TENTLER, T. 2005. Propagation of brittle failure triggered by magma in Iceland. *Tectonophysics*, **406**, 17–38.

THYBO, H., MAGUIRE, P., BIRT, C. & PERCHUC, E. 2000. Seismic reflectivity and magmatic underplating beneath the Kenya Rift. *Geophysical Research Letters*, **27**, 2745–2748.

TONGUE, J., MAGUIRE, P. & BURTON, P. 1994. An earthquake study in the Lake Baringo basin of the central Kenya Rift. *Tectonophysics*, **236**, 151–164.

TUCKWELL, G., BULL, J. & SANDERSON, D. 1996. Models of fracture orientation at oblique spreading centres. *Journal of the Geological Society, London*, **153**, 185–189, http://doi.org/10.1144/gsjgs.153.2.0185

VAUCHEZ, A., DINEUR, F. & RUDNICK, R. 2005. Microstructure, texture and seismic anisotropy of the lithospheric mantle above a mantle plume: insights from the Labait volcano xenoliths (Tanzania). *Earth and Planetary Science Letters*, **232**, 295–314.

VERSFELT, J. & ROSENDAHL, B. 1989. Relationships between pre-rift structure and rift architecture in Lakes Tanganyika and Malawi, East Africa. *Nature*, **337**, 354–357.

WALLMANN, P. C., POLLARD, D. D., HILDRETH, W. & EICHELBERGER, J. C. 1990. New structural limits on magma chamber locations at the Valley of Ten Thousand Smokes, Katmai National Park, Alaska. *Geology*, **18**, 1240–1243.

WEAVER, S. 1977. The Quaternary caldera volcano Emuruangogolak, Kenya Rift, and the petrology of a bimodal ferrobasalt-pantelleritic trachyte association. *Bulletin Volcanologique*, **40**, 209–230.

WILLIAMS, H. 1941. *Calderas and their Origin*. University of California Press, Oakland.

WILLIAMS, L. A. J. 1978a. The volcanological development of the Kenya Rift. *In*: NEUMANN, E.-R. & RAMBERG, I. B. (eds) *Petrology and Geochemistry of Continental Rifts*. Springer, the Netherlands, 101–121.

WILLIAMS, L. A. J. 1978b. Character of Quaternary volcanism in the Gregory Rift Valley. *In*: BISHOP, W. W. (ed.) *Geological Background to Fossil Man: Recent Research in the Gregory Rift Valley, East Africa*. Geological Society, London, Special Publications **6**, 55–69, http://doi.org/10.1144/GSL.SP.1978.006.01.06

WILLIAMS, L. A. J., MACDONALD, R. & CHAPMAN, G. 1984. Late Quaternary caldera volcanoes of the Kenya Rift valley. *Journal of Geophysical Research*, **89**, 8553–8570.

WILSON, C., HOUGHTON, B., MCWILLIAMS, M., LANPHERE, M., WEAVER, S. & BRIGGS, R. 1995. Volcanic and structural evolution of Taupo Volcanic Zone, New Zealand: a review. *Journal of Volcanology and Geothermal Research*, **68**, 1–28.

WOOLLEY, A. R. (ed.) 2001. *Alkaline Rocks and Carbonatites of the World: Part 3: Africa*. Volume **3**. Geological Society, London.

WORMALD, S. C., WRIGHT, I. C., BULL, J. M., LAMARCHE, G. & SANDERSON, D. J. 2012. Morphometric analysis of the submarine arc volcano Monowai (Tofua–Kermadec Arc) to decipher tectono-magmatic interactions. *Journal of Volcanology and Geothermal Research*, **239–240**, 69–82.

YOUNG, P., MAGUIRE, P., LAFFOLEY, N. D. & EVANS, J. 1991. Implications of the distribution of seismicity near Lake Bogoria in the Kenya Rift. *Geophysical Journal International*, **105**, 665–674.

ZOBACK, M. D., ZOBACK, M. L. *ET AL.* 1987. New evidence on the state of stress of the San Andreas fault system. *Science*, **238**, 1105–1111.